

**Best Available  
Copy  
for all Pictures**

AD-778 685

INTERACTION BETWEEN AMORPHOUS  
SEMICONDUCTOR THIN FILM AND ELECTRON  
BEAM

Arthur C. M. Chen

General Electric Corporate Research and  
Development

Prepared for:

Army Research Office-Durham  
Advanced Research Projects Agency

April 1974

DISTRIBUTED BY:

**NTIS**

National Technical Information Service  
U. S. DEPARTMENT OF COMMERCE  
5285 Port Royal Road, Springfield Va. 22151

AD778685

# INTERACTION BETWEEN AMORPHOUS SEMICONDUCTOR THIN FILM AND ELECTRON BEAM

Arthur C. M. Chen

General Electric Corporate Research and Development  
Schenectady, New York  
Telephone: AC518-346-8771

FINAL TECHNICAL REPORT, APRIL 1974

Contract No: DAHC 04-72-C-0016  
ARPA Order No: 1562, Amendment 3  
Program Code No: 61101E

Period of Contract: February 7, 1972 to December 31, 1973

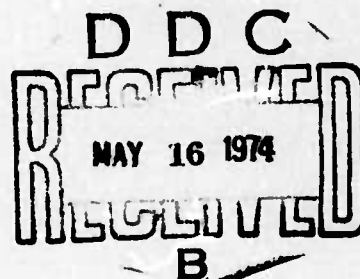
Amount of Grant/Contract \$64,382

Prepared For

U. S. Army Research Office  
Durham, North Carolina 27703

and

Advanced Research Projects Agency  
Arlington, Virginia 22209



Approved for public release; distribution unlimited

The views and conclusions contained in this document are those of the authors and should not be interpreted as necessarily representing the official policies, either expressed or implied, of the advanced Research Projects Agency or the U. S. Government

NATIONAL TECHNICAL  
INFORMATION SERVICE  
U. S. Department of Commerce  
Springfield VA 22151

SRD-74-041

ib

## TECHNICAL SUMMARY

This is the final technical report on the research program, "Interaction Between Amorphous Semiconductor Thin Film and Electron Beam," sponsored by the U. S. Army Research Office and the Advanced Research Projects Agency under contract DAHC 04-72-C-0016. The period of the contract was February 7, 1972 to December 31, 1973. This report summarizes the research conducted during the above period. In particular, the detailed results during the period from May 7, 1973 to December 31, 1973 are reported here.

Our first year of research has led to a good understanding of the physical basis which determines the potential performance characteristics of an amorphous semiconductor electron beam memory.

Our effort during the second year has been to determine quantitatively the factors, electron beam readout and write sensitivities, which are crucial to the memory performance characteristics.

We have extended our understanding of the nature of electron beam readout sensitivity. In addition, an extensive series of measurements of this sensitivity on a range of Ge-based amorphous semiconductor thin films has been made. These results enabled us to map out the potential performance regions of this type of electron beam memory. These measurements and their implication on the memory performance are reported here.

Finally we have attempted to determine the possible enhancement of the write or the crystallization process in these films by the electronic nature of the electron beam. We have devised a unique experiment to measure the influence of electron beam on  $T_x$ , the crystallization temperature. Our results on  $\text{Ge}_{37}\text{Te}_{69}\text{As}_3$  were negative. But, because of various experimental factors which may influence our results, we can only tentatively conclude that in the film we studied, the influence of electron beam on  $T_x$ , if any, is small.

## TABLE OF CONTENTS

<u>Section</u>	<u>Page</u>
TECHNICAL SUMMARY	iii
LIST OF ILLUSTRATIONS	vii
I. INTRODUCTION	1
II. ELECTRON BEAM READOUT SENSITIVITY OF Ge-Te-X AMORPHOUS SEMICONDUCTOR THIN FILMS	3
A. Theory of Electron Beam Readout Sensitivity	3
B. Experimental Results	5
III. A STUDY OF POSSIBLE ELECTRON BEAM ENHANCEMENT OF CRYSTALLIZATION PROCESS IN AMORPHOUS SEMICONDUCTOR THIN FILMS	21
A. Experimental Technique	21
B. Electron Beam Test Cell	24
C. Experimental Results	30
IV. PARTICIPATING PERSONNEL	33
PUBLICATION	33
REFERENCES	33

## LIST OF ILLUSTRATIONS

### Figure

- 1 - Pictorial representation of the electron beam readout process. Left half, amorphous semiconductor thin film target; right half, metallic film covered target.
- 2 - The readout sensitivity of  $\text{Ge}_{15}\text{Te}_{81}\text{As}_4$  assuming a surface deformation of  $25^\circ$ .
- 3 - The readout sensitivity of  $\text{Ge}_{37}\text{Te}_{80}\text{As}_3$  assuming a surface deformation of  $25^\circ$ .
- 4 - The readout sensitivity of flash evaporated film of  $\text{Ge}_{4.8}\text{Te}_{78}\text{As}_{17.2}$ . Assumed surface deformation,  $25^\circ$ .
- 5 - Electron beam readout sensitivity of  $\text{Ge}_{15}\text{Te}_{81}\text{As}_4$  thin films for various surface deformations.
- 6 - Electron beam readout sensitivity of  $\text{Ge}_{15}\text{Te}_{81}\text{Sb}_4$  thin films for various surface deformations.
- 7 - Electron beam readout sensitivity of  $\text{Ge}_{37}\text{Te}_{80}\text{As}_3$  thin films for various surface deformations.
- 8 - Electron beam readout sensitivity of  $\text{Ge}_{33}\text{Te}_{87}$  thin films for various surface deformations.
- 9 - Electron beam readout sensitivity of  $\text{Ge}_{4.8}\text{Te}_{78}\text{As}_{17.2}$  thin films for various surface deformations.
- 10 - Electron beam readout sensitivity of  $\text{Ge}_{10}\text{Se}_{80}\text{As}_{40}$  thin films for various surface deformations.
- 11 - Electron beam readout sensitivity of Mo thin films for various surface deformations.
- 12 - The readout sensitivity of Ge-based thin films for surface deformation of  $10^\circ$ .
- 13 - The readout sensitivity of Ge-based thin films for surface deformation of  $25^\circ$ .
- 14 - The readout sensitivity of Ge-based thin films for surface deformation of  $40^\circ$ .

## LIST OF ILLUSTRATIONS (Cont'd)

### Figure

- 15 - Nomograph of the performance characteristics of amorphous semiconductor electron beam memory. The dashed hatched area is the possible performance region for target readout; the oval hatched region is for secondary electron readout.
- 16 - The schematic of the Resistance vs. Temperature measuring apparatus. The measured Log R vs. T curve shows a  $T_x$  of 246°C for this film.
- 17 - Special amorphous semiconductor thin film resistor structure for electron beam crystallization experiment. Electron is scanned over only the larger of the two series resistors.
- 18 - Possible Log R vs. T characteristics for electron beam induced decrease in  $T_x$  for sample in Figure 17.
- 19 - Two electron sources used in this research program. Foreground, high brightness ThC electron gun. Background, tungsten filament electron gun.
- 20 - Oscilloscope traces of modulation input (top, 40v) and the electron beam output from target current amplifier (bottom, 2.5  $\mu$ A). Horizontal scale; 5  $\mu$ s/cm (top); 100 ns/cm (bottom).
- 21 - Schematic of the high vacuum heated sample stage for Log R vs. T measurement.
- 22 - Photograph of the high vacuum sample stage. The two disks next to the resistor sample are the target grids used for electron beam focus adjustment.
- 23 - Video signal from the 200 mesh grid used for electron beam focus adjustment.
- 24 - The electron beam test cell with the resistance vs. temperature measurement apparatus.

# INTERACTION BETWEEN AMORPHOUS SEMICONDUCTOR THIN FILM AND ELECTRON BEAM

Arthur C. M. Chen

## I. INTRODUCTION

This is the final technical report on the research program, "Interaction Between Amorphous Semiconductor Thin Film and Electron Beam," sponsored by the U. S. Army Research Office, and the Advanced Research Projects Agency, Arlington, Va. under contract DAHC 04-72-C-0016. The report describes the research conducted during the period February 7, 1972 to Dec. 31, 1973.

The original objective of the program was to gain an increased understanding of the "switching" properties of amorphous semiconductor thin films by the use of electron beam as a diagnostic tool. However, during the course of our investigation, it appeared that the amorphous to crystalline phase transition phenomenon in these thin films is an excellent candidate as a storage mechanism in an electron beam computer memory device - in particular, as a large archival mass memory. Because of the potential application importance of the above device, the research program scope had been enlarged to encompass a study of the possible device and system characteristics of an amorphous semiconductor electron beam memory.

In our first year of this research program, we have extended our original work on secondary electron emission from amorphous semiconductor to gain important insights into the physics of the electron beam recording, "writing and reading", processes in amorphous semiconductor thin films. These works are reported in references (1), (2) and (3). In addition during this period we had developed a very good qualitative understanding of the possible computer memory and system characteristics of amorphous semiconductor electron beam memory. These characteristics, in particular their performance limitations, are based upon certain basic physical constraints on any electron beam devices as well as upon certain estimated parameters of electron beam-amorphous semiconductor thin film interactions. Based upon some preliminary experiments, we have shown that amorphous semiconductor electron beam memory in a read-only archival mode can achieve bit density of  $10^9$  bits/in<sup>2</sup> with readout data rate in excess of 20 m bits/sec. The detailed technical analyses of these results are described in the first semiannual technical report of this research program.

One further result of our first year's work was the identification of the need to know quantitatively the characteristics of electron beam writing and reading processes in various amorphous semiconductor films. With these quantitative results, we can determine more precisely the possible electron



beam memory characteristics as well as to aid in the possible fruition of this device. Thus our second year was aimed at the measurement of electron beam read-out sensitivity of amorphous semiconductor thin films. In addition, we initiated an effort to determine the nature, if any, of possible electron beam enhancement of the crystallization process in these films. Both of these research efforts required the development of new measurement techniques and the construction of new apparatus. The results will be summarized in this report.

During the course of our experimental work it was necessary to develop a reproducible amorphous semiconductor thin film deposition process. In this development we have investigated the influence of RF sputtering process and the possible thickness dependence of the crystallization temperature of Ge-Te-As thin films. The influence of sputtering target preparation in inducing Te deficiency in the resultant film was determined. In addition, for film thickness of less than  $0.7\mu$ , there is an increase in the crystallization temperature. This latter effect can have an influence on possible device characteristics. The details of these investigations were reported in our second semiannual technical report.

One result of our research program has been to identify and to understand the basic mechanism and performance limitation of possible amorphous semiconductor electron beam memory. In this understanding, it has implicitly recognized the importance of allied technologies such as electron beam source, electron optics and material preparation in making such a device possible. The requirements on these allied technologies will push the state-of-the-art in these areas. Thus to bring the amorphous semiconductor electron beam memory to fruition will require not only advances in amorphous semiconductor technology but also in the above allied technologies. However, with the present research progress in all these areas, one can foresee the realization of such a device in the near future to meet the increasing need of large on-line mass memory in computer systems.

UNCLASSIFIED

Security Classification

AD-778685

## DOCUMENT CONTROL DATA - R &amp; D

(Security classification of title, body of abstract and indexing annotation must be entered when the overall report is classified)

1. ORIGINATING ACTIVITY (Corporate author)

General Electric Research and Development Center  
Schenectady, New York

2a. REPORT SECURITY CLASSIFICATION

Unclassified

2b. GROUP

3. REPORT TITLE

INTERACTION BETWEEN AMORPHOUS SEMICONDUCTOR THIN  
FILM AND ELECTRON BEAM

4. DESCRIPTIVE NOTES (Type of report and inclusive dates)

Final Technical Report Feb. 7, 1972 to Dec. 31, 1973

5. AUTHOR(S) (First name, middle initial, last name)

Arthur C. M. Chen

6. REPORT DATE

December 31, 1973

7a. TOTAL NO. OF PAGES

42

7b. NO. OF REFS

9

8a. CONTRACT OR GRANT NO.

DAHC 04-72-C-0016

b. PROJECT NO.

9a. ORIGINATOR'S REPORT NUMBER(S)

SRD-74-041

c.

9b. OTHER REPORT NO(S) (Any other numbers that may be assigned  
this report)

d.

10. DISTRIBUTION STATEMENT

Approved for public release; distribution unlimited

11. SUPPLEMENTARY NOTES

12. SPONSORING MILITARY ACTIVITY

U.S. Army Research Office  
Durham, North Carolina 27706 and  
Advanced Research Projects Agency  
Arlington, Virginia 22209

13. ABSTRACT

This is the final technical report on the research program, "Interaction Between Amorphous Semiconductor Thin Film and Electron Beam," sponsored by the U. S. Army Research Office and the Advanced Research Projects Agency under contract DAHC 04-72-C-0016. The period of the contract was February 7, 1972 to December 31, 1973. This report summarizes the research conducted during the above period. In particular, the detailed results during the period from May 7, 1973 to December 31, 1973 are reported here.

Our first year of research has led to a good understanding of the physical basis which determines the potential performance characteristics of an amorphous semiconductor electron beam memory.

Our effort during the second year has been to determine quantitatively the factors, electron beam readout and write sensitivities, which are crucial to the memory performance characteristics.

We have extended our understanding of the nature of electron beam read-out sensitivity. In addition, an extensive series of measurements of this sensitivity on a range of Ge-based amorphous semiconductor thin films has been made. These results enabled us to map out the potential performance regions of this type of electron beam memory. These measurements and their implication on the memory performance are reported here.

Finally we have attempted to determine the possible enhancement of the write or the crystallization process in these films by the electronic nature of the electron beam. We have devised a unique experiment to measure the influence of electron beam on  $T_x$ , the crystallization temperature. Our results on  $\text{Ge}_3\text{Te}_{99}\text{As}_2$  were negative. But, because of various experimental factors which may influence our results, we can only tentatively conclude that in the film we studied, the influence of electron beam on  $T_x$ , if any, is small.

Reproduced by  
NATIONAL TECHNICAL  
INFORMATION SERVICE  
U S Department of Commerce  
Springfield VA 22151

DD FORM 1 NOV 65 1473

UNCLASSIFIED

Security Classification

UNCLASSIFIED

Security Classification

ia

14. KEY WORDS	LINK A		LINK B		LINK C	
	ROLE	WT	ROLE	WT	ROLE	WT
Amorphous Semiconductor Electron Beam Memory Secondary Electron Emission						

UNCLASSIFIED

Security Classification

ia

## II. ELECTRON BEAM READOUT SENSITIVITY OF Ge-Te-X AMORPHOUS SEMICONDUCTOR THIN FILMS

One main effort during the second year of the research program has been the completion of our extensive investigation of electron beam readout sensitivity of Ge-Tx-X amorphous films to identify the possible range of behavior of this important parameter. This section will summarize our findings.

### A. Theory of Electron Beam Readout Sensitivity

The elementary ideas of the electron beam writing and reading process described two years ago<sup>(1)</sup> have undergone considerable modifications in light of our present knowledge. The electron beam recording process is pictorially shown in Figure (1) where we have split the figure into two halves to show two possible implementations. The writing process uses the electron beam to heat and to crystallize the amorphous thin film. These crystalline spots define the "1" state of the memory. In addition, information is also stored as the deformation which accompanied this phase transformation.

On the left side of Figure 1 is shown one possible target implementation in which the surface of the amorphous film acts as the storage medium. Without any crystalline recording, the secondary electron emission is given by  $\delta^0 I_p$ . With crystalline recording, the secondary electron emission is altered<sup>a</sup> by the change in the secondary yield and the surface deformation and is designated by  $\delta_c(\theta) I_p$ .

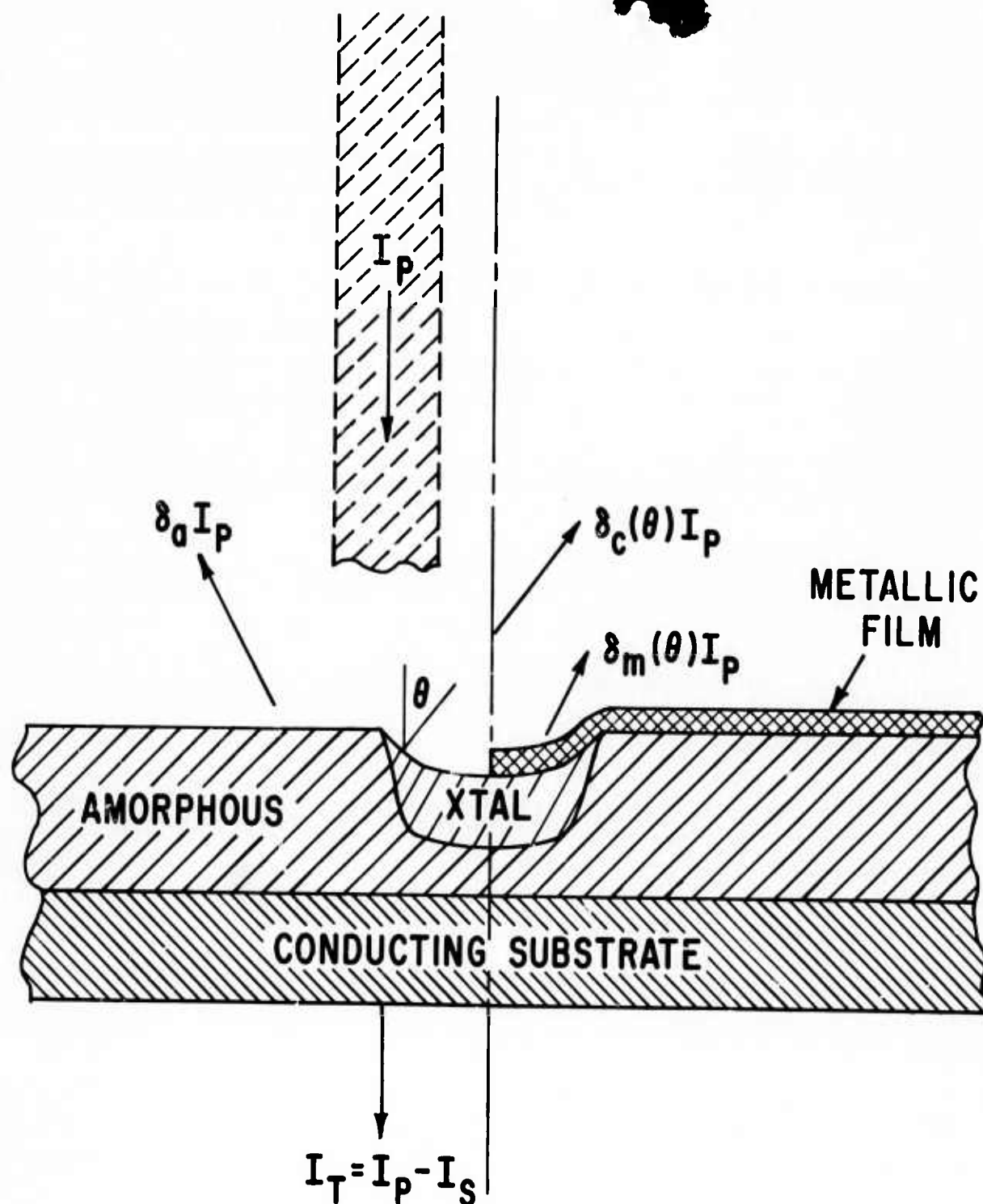
On the right side of Figure 1 is shown the second possible target implementation in which the amorphous film is covered by a thin ( $\sim 100\text{\AA}$ ) metallic film before any recording takes place. In this case, the crystalline recordings are read out by the change in surface deformation alone and the secondary electron emission is given by  $\delta_m(\theta) I_p$ .

With the above physics of the recording process, we can define an electron beam readout sensitivity function

$$S_T(\theta, V) = \frac{\delta^1 - \delta^0}{\delta^0} \quad (1)$$

where 1 and 0 denote "1" and "0" state of the memory. In general, the 1/0 readout ratio of the memory will be given by

$$\frac{1}{0} = \left| \int_A S_T(\theta, V) J_p dA \right| \quad (2)$$



## ELECTRON BEAM READOUT SENSITIVITY

Figure 1 Pictorial representation of the electron beam readout process. Left half, amorphous semiconductor thin film target; right half, metallic film covered target.

where  $J_p$  is the primary current density and the integral is taken over the area of the recording.  $S_T$  will depend on  $\theta$  as well as on the beam voltage,  $V$ .

$S_T(\theta, V)$  is the sum of two parts,  $S_1$  and  $S_2$ . The first part is due to the change in secondary electron yield between the amorphous and the crystalline phase with normal incidence primary electron beam. It is given by

$$S_1 = \left[ \frac{\delta_a - \delta_a}{\delta_a} \right]_{\theta=0} \quad (3)$$

where  $c$  and  $a$  describe the crystalline and the amorphous phases. The second part describes the readout process due to surface deformation of the crystalline phase alone. It is given by

$$S_2 = \left[ \frac{\delta_\theta - \delta_o}{\delta_o} \right]_{\text{crystalline}} \quad (4)$$

where  $\theta$  and  $o$  denote oblique and normal incidence of the primary beam. Based upon some elementary considerations, and experimentally verified results<sup>(4)</sup>  $S_2$  has shown to be

$$S_2 = e^{k(1-\cos \theta)} - 1 \quad (5)$$

where  $k$  is the secondary electron angular coefficient. It is equal to the product of the secondary electron absorption coefficient and its mean depth of escape. As  $k > 0$ ,  $S_2$  is always positive. However  $S_1$  may be negative if  $\delta_a > \delta_c$ . In this case  $S_1$  and  $S_2$  are self cancelling and result in a smaller net positive or negative value for  $S(\theta, V)$ . However it should be noted that it is  $|S_T(\theta, V)|$ , the magnitude of  $S_T$ , that is important for memory operation.

## B. Experimental Results

To determine the readout sensitivity of various Ge-based amorphous thin films, we have constructed an ultra high vacuum apparatus for measuring the secondary electron yield at various beam voltages and angles. This apparatus and the experimental techniques were described in our previous report.<sup>(5)</sup> The films were all about 5000Å thick on oxidized Si substrates. They were prepared by RF sputtering process. The compositions were determined by microprobe analysis and are listed in the table below.

### Composition Analysis of the Ge-based Films

<u>Nominal</u>	<u>Analysis</u>
$\text{Ge}_{15}\text{Te}_{81}\text{As}_4$	$\text{Ge}_{14.3}\text{Te}_{81.5}\text{As}_{4.2}$
$\text{Ge}_{15}\text{Te}_{81}\text{Sb}_4$	$\text{Ge}_{17.8}\text{Te}_{79.3}\text{Sb}_{2.9}$
$\text{Ge}_{37}\text{Te}_{80}\text{As}_3$	$\text{Ge}_{42.6}\text{Te}_{54.9}\text{As}_{2.5}$
$\text{Ge}_{37}\text{Te}_{87}$	$\text{Ge}_{40}\text{Te}_{80}$
$\text{Ge}_5\text{Te}_{78}\text{As}_{17}$	$\text{Ge}_{4.8}\text{Te}_{78}\text{As}_{17.2}$

One result is that  $k$  was similar in value for the various Ge-based films we measured. This is probably because the films have similar atomic weight and density.

More generally, Ge-based amorphous films have shown that a wide variation in readout characteristics is possible. Depending on the relative change in the secondary yield between the amorphous and the crystalline phase, the readout characteristics ranged from large negative to nearly zero to large positive sensitivity.

For example,  $\text{Ge}_{15}\text{Te}_{81}\text{As}_4$  has a large positive increase in the secondary yield as the film is transformed from the amorphous to the crystalline phase. Thus  $S_1$  is positive and makes a significant contribution to the readout sensitivity as shown in Figure 2. Here we have assumed a surface deformation of  $25^\circ$ .

On the other hand,  $\text{Ge}_{37}\text{Te}_{80}\text{As}_3$ , which is a candidate for possible archival memory applications, exhibits almost no change in the secondary yield between the two phases. In this case the readout sensitivity is almost entirely due to  $S_2$  alone as shown in Figure 3. Again, a deformation of  $25^\circ$  has been assumed.

Finally, some of our earlier flash evaporated films<sup>(1)</sup> exhibited higher yield in the amorphous phase than in the crystalline phase. In this case  $S_1$  would be negative and would partially cancel the effect of the surface deformation,  $S_2$ , as shown in Figure 4.

The experimentally measured  $S_1$ ,  $S_2$  and  $S_T$  for various Ge-Te based amorphous semiconductor films at  $10^\circ$ ,  $25^\circ$  and  $40^\circ$  are shown in Figures 5, 6, 7, 8 and 9. Figure 10 shows the result for a Ge-Se based film,  $\text{Ge}_{10}\text{Se}_{50}\text{As}_{40}$ , which we briefly examined for photo-crystallization phenomenon. This film was made from RF sputtering target purchased from a commercial firm and the film composition was not subjected to microprobe analysis.



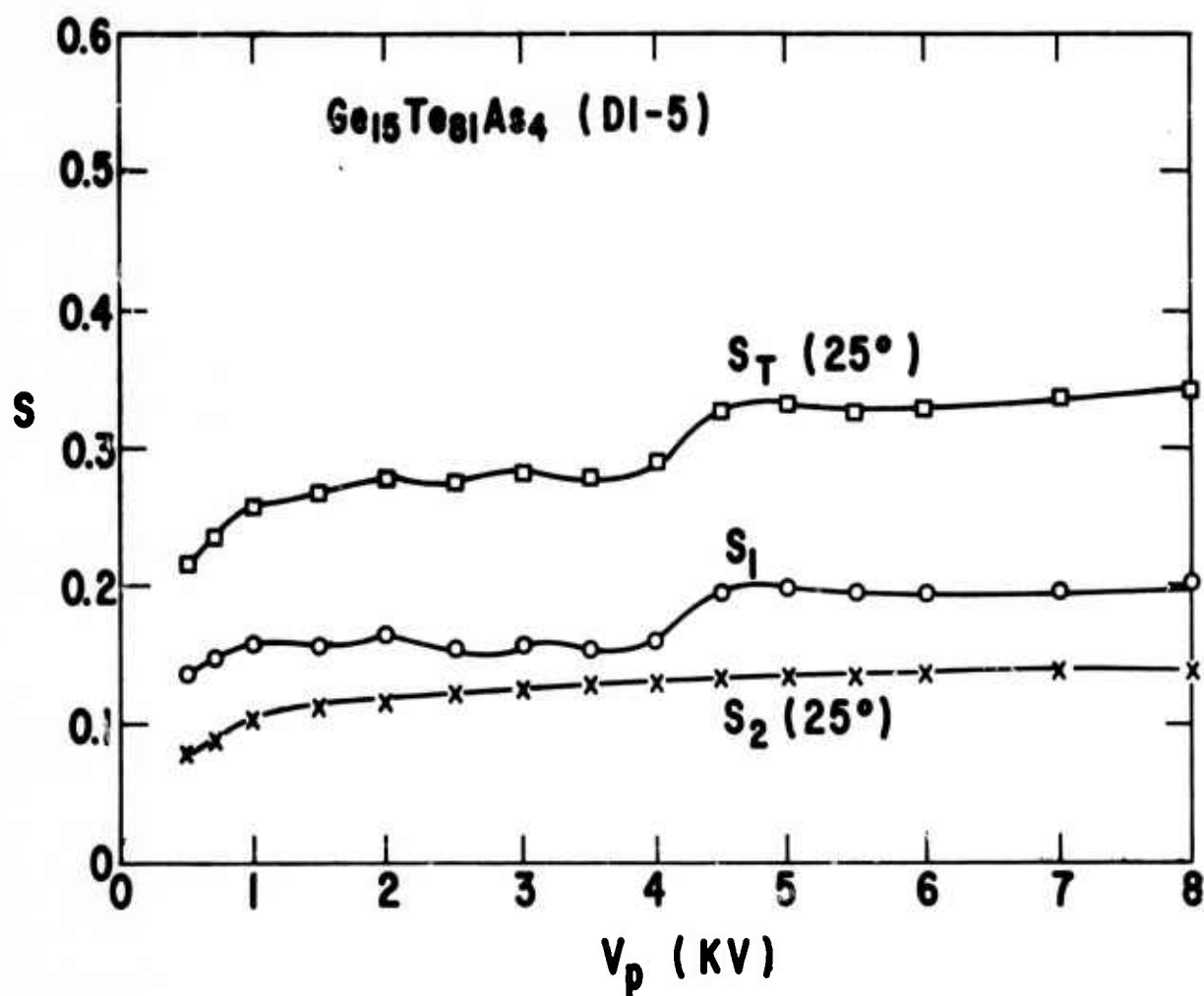


Figure 2 The readout sensitivity of  $\text{Ge}_{15}\text{Te}_{81}\text{As}_4$  assuming a surface deformation of  $25^\circ$ .

To evaluate quantitatively the two possible implementations of amorphous semiconductors as a memory target shown in Figure 1, the readout sensitivity of Mo thin film was also measured in the same apparatus. The film was prepared by RF sputtering. To prevent possible extraneous results from being induced by the film substrate, the Mo film thickness was about  $6000\text{\AA}$ . Its electron beam readout sensitivity is shown in Figure 11. The readout sensitivity would be due to surface deformation alone as the Mo covered amorphous semiconductor memory target will have  $S_1 = 0$ . The above results are summarized in Figures 12, 13 and 14 for  $\theta = 10^\circ$ ,  $25^\circ$  and  $40^\circ$  respectively.

In an amorphous semiconductor electron beam memory, the surface deformation which accompanies the "writing" or the crystallization process is expected to be strongly dependent on the electron beam induced thermal profile during the writing process. Thus a sharp and well defined beam



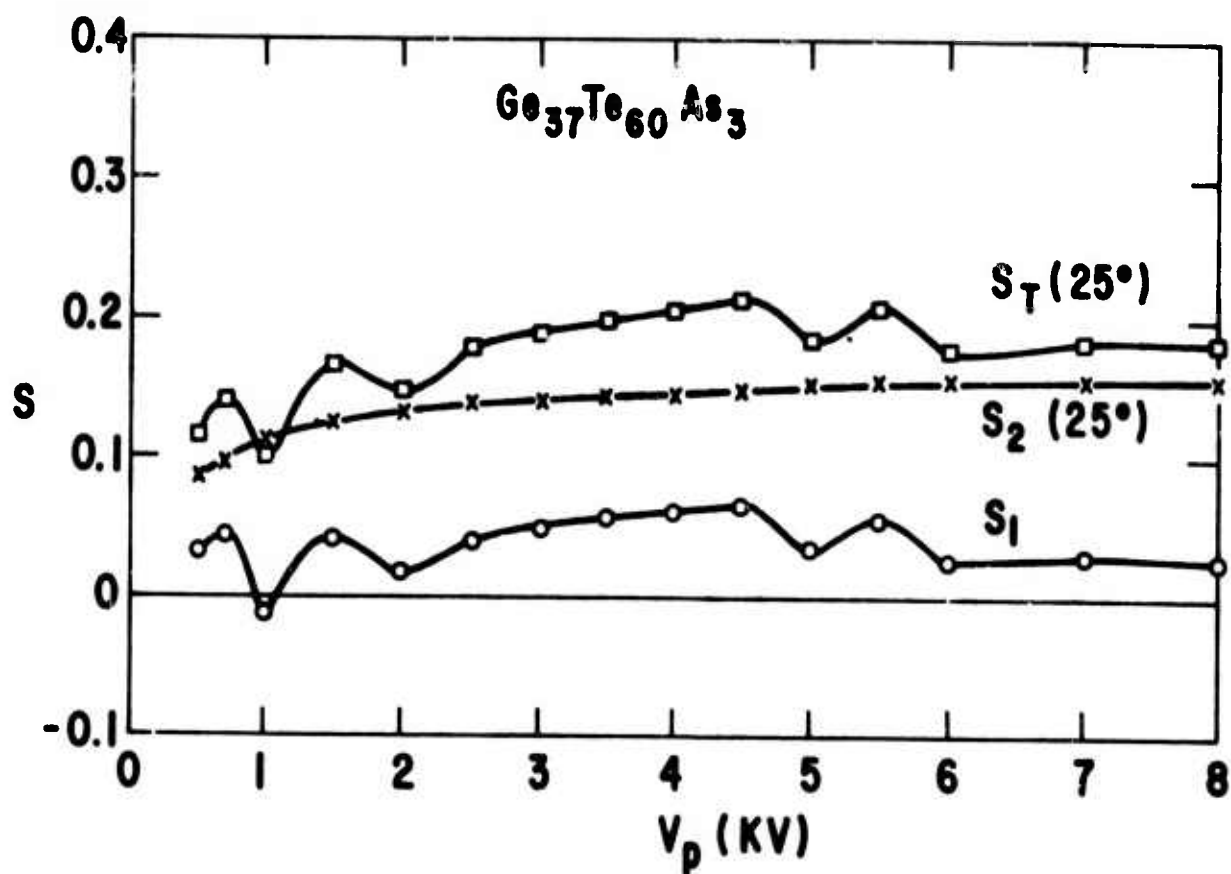


Figure 3 The readout sensitivity of  $\text{Ge}_{37}\text{Te}_{60}\text{As}_3$  assuming a surface deformation of  $25^\circ$ .

profile can induce a large surface deformation. On the other hand, a poorly defined beam profile will cause only a small deformation.

Our results show that at small deformations, i. e. Figure 12,  $\theta = 10^\circ$ , the readout sensitivity is small but still adequate for electron beam memory application. As expected, at small angle, the contribution of the change in secondary electron emission between the amorphous and crystalline phase dominates the total readout sensitivity,  $S_T$ . Note the small  $S_T$  for Mo as compared to other uncovered Ge based films in Figure 12. However, at high deformation angles, i. e.  $\theta = 40^\circ$ , the enhancement of secondary yield at oblique incident angle dominates the readout sensitivity as evidence by the results summarized in Figure 14.

With these measured readout sensitivities of a wide variety of Ge-based films, we are in a better position to evaluate the possible performance characteristics of amorphous semiconductor electron beam memory. Our previous system consideration has shown that the memory characteristics are constraint by two relationships.<sup>(6, 7)</sup>

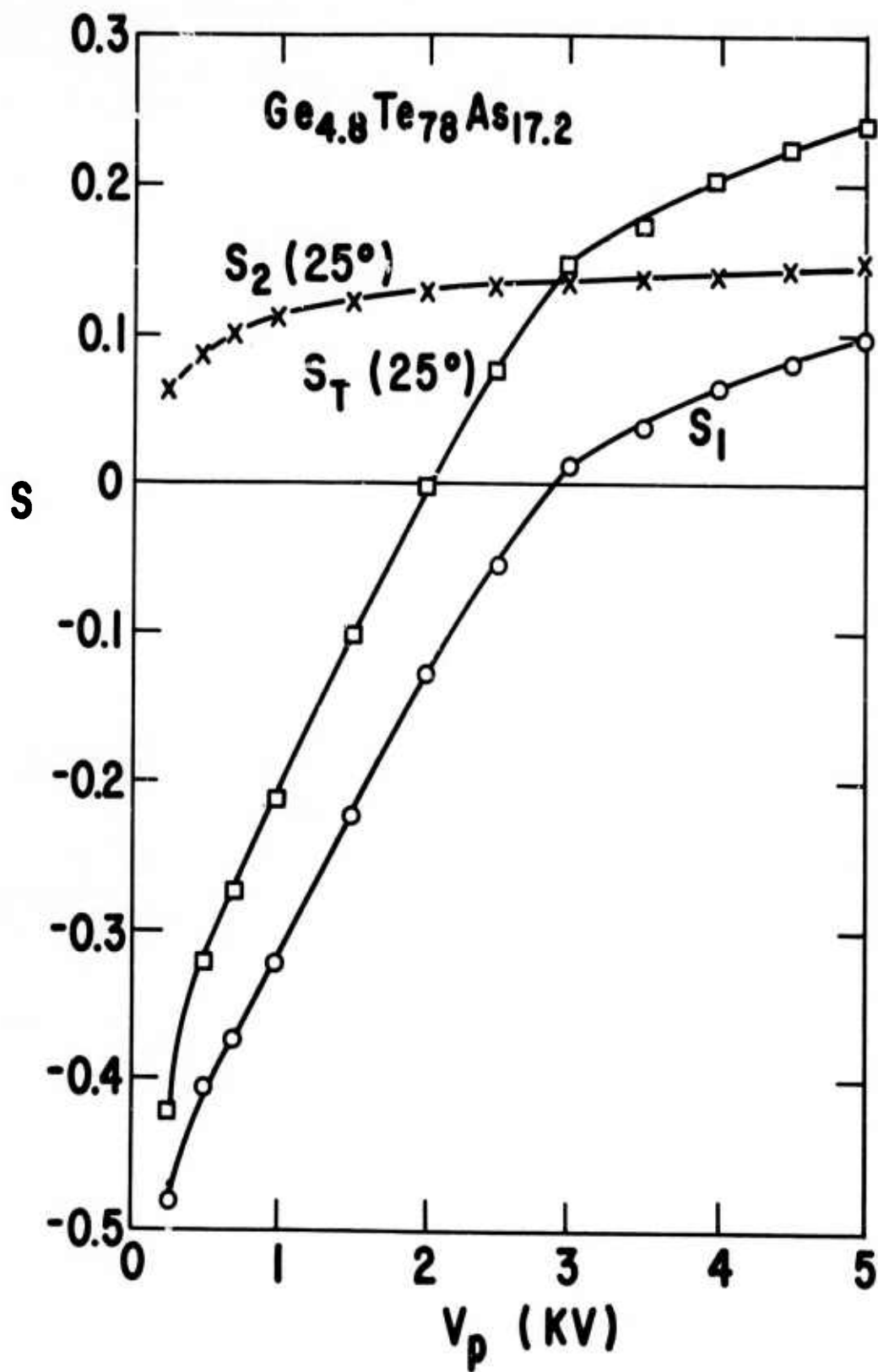


Figure 4 The readout sensitivity of flash evaporated film of  $\text{Ge}_{4.8}\text{Te}_{7.8}\text{As}_{17.2}$ . Assumed surface deformation,  $25^\circ$ .

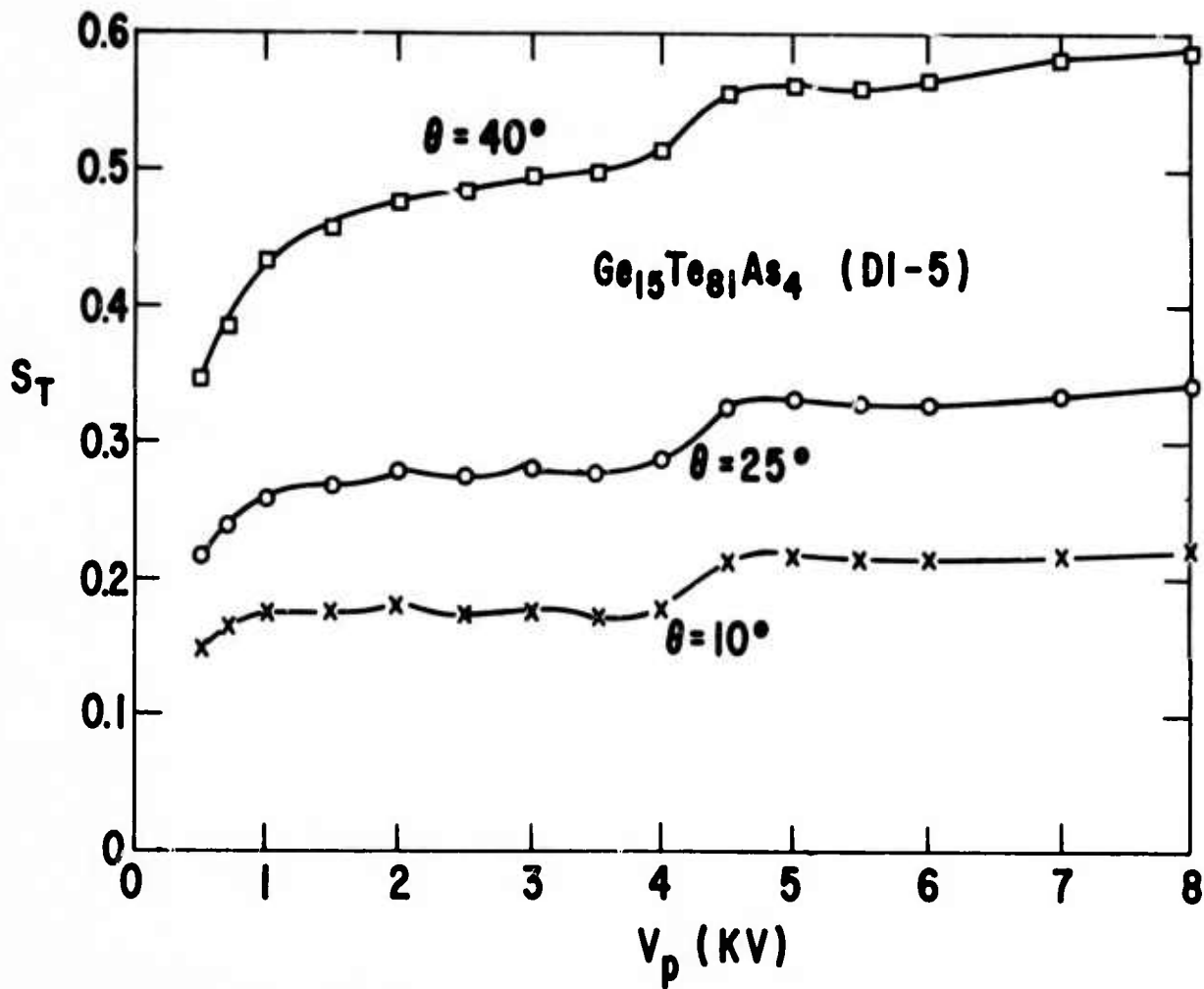


Figure 5 Electron beam readout sensitivity of  $\text{Ge}_{15}\text{Te}_{81}\text{As}_4$  thin films for various surface deformation.

The first relationship is the minimum primary beam current needed to fulfill the signal to noise requirement to obtain an acceptable low error rate needed for practical memory applications. This relationship takes two forms depending on the signal detection process. They are: (6)

$$I_p > \frac{1}{M^2} \left( \frac{S}{N} \right)^2 2eb\delta\Delta f \quad (6)$$

for secondary electron detection

and 
$$I_p > \frac{I}{M} \left( \frac{S}{N} \right) (\delta\pi kT C_T)^{1/2} \Delta f \quad (7)$$

for target current detection.

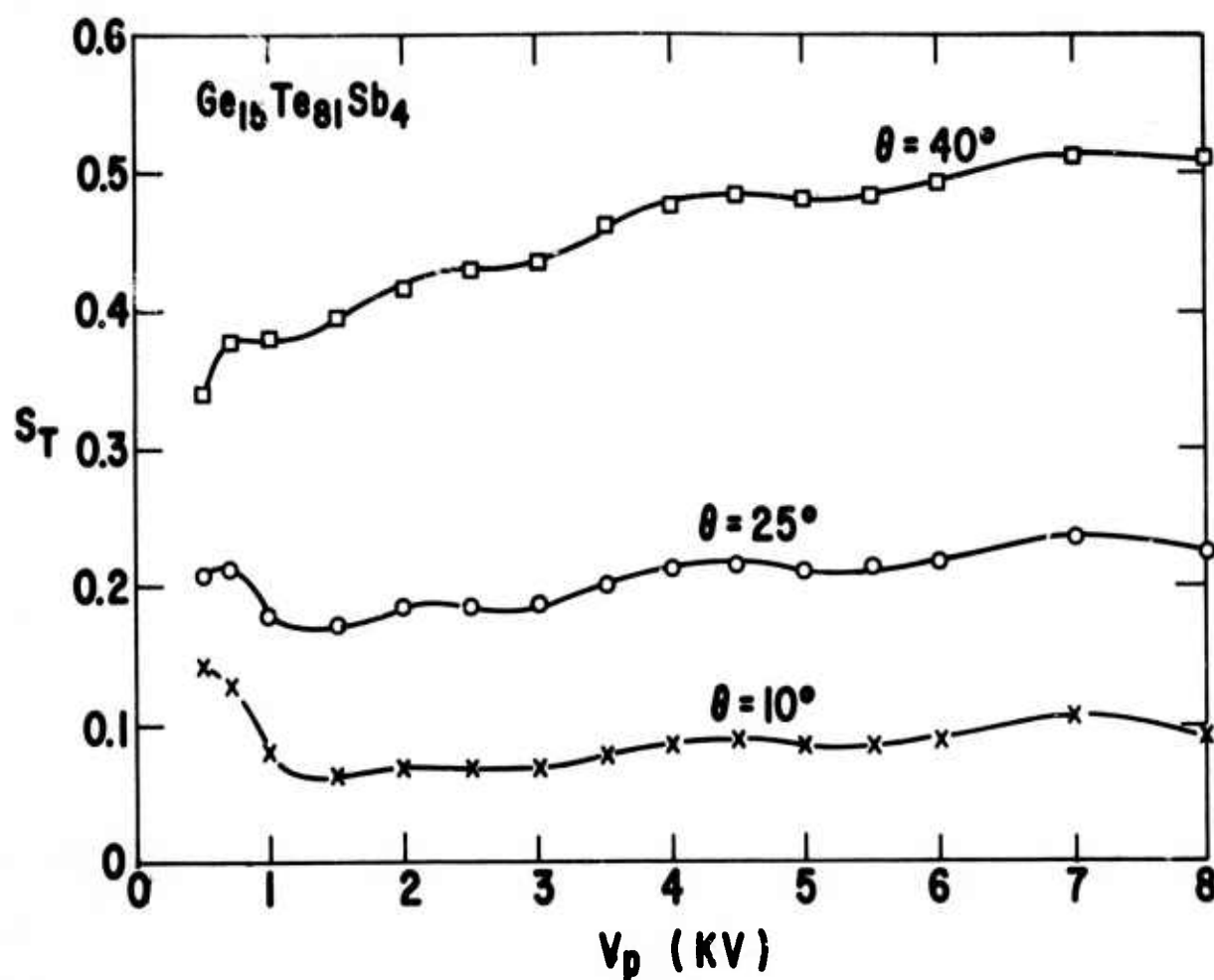


Figure 6 Electron beam readout sensitivity of  $\text{Ge}_{15}\text{Te}_{81}\text{Sb}_4$  thin films for various surface deformations.

$I_p$  is the primary beam current,  $(S/N)$  is the signal to noise ratio,  $\delta$  is the average yield,  $\Delta f$  is the bandwidth,  $b$  is a constant which expresses the possible fluctuation in secondary yield of the target and  $C_T$  is the target capacitance.  $M$  was defined to be the modulation coefficient and is equal to  $\delta^0 S_T$  where  $\delta^0$  is the yield of the "0" state.

The second relationship is the limitation on the primary current imposed by the Langmuir's limit and spherical aberration of electron-optic system. (7) This limitation is given by the relationship,

$$I_{p \max} < \frac{3\pi}{16} j_0 \left( \frac{eV}{kT} \right) d^2 \alpha_{ax}^2 \quad (8)$$

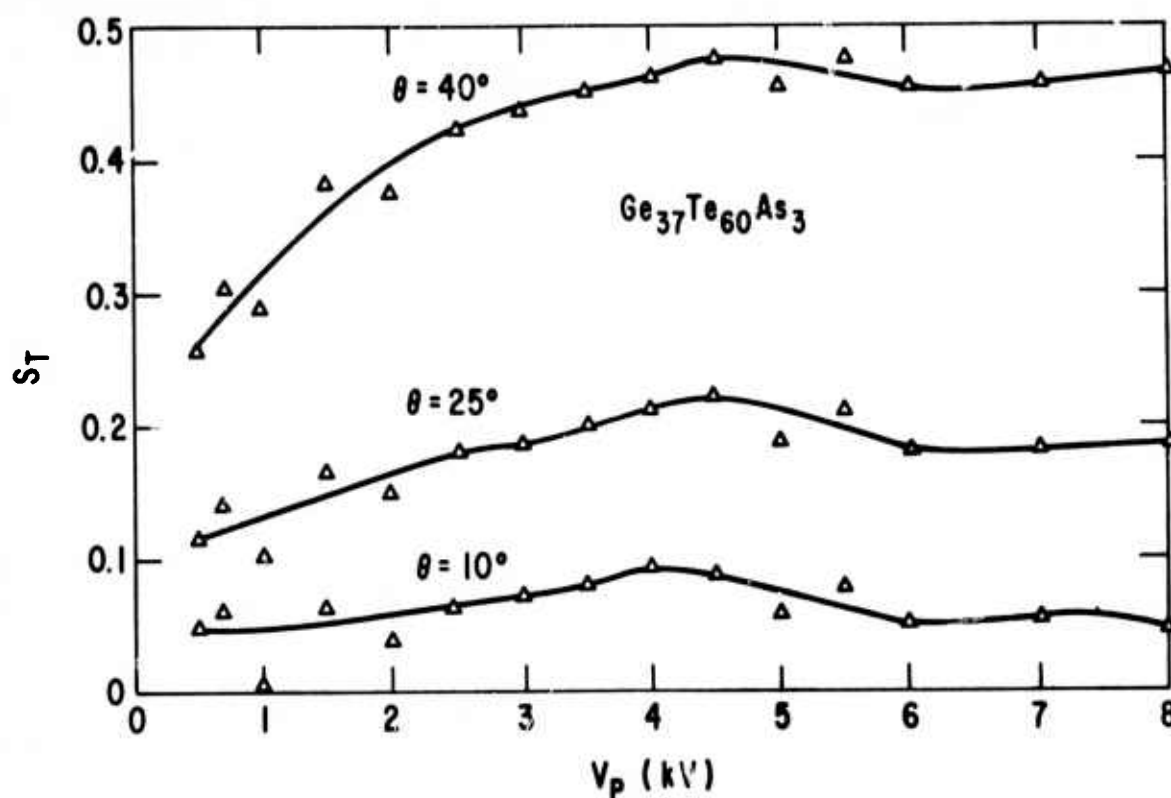


Figure 7 Electron beam readout sensitivity of  $\text{Ge}_{37}\text{Te}_{60}\text{As}_3$  thin films for various surface deformations.

where

$$\alpha_{\max}^3 = \left( \frac{d}{C_s} \right) \quad (9)$$

is the maximum half-angle of the converging beam.  $C_s$  is the spherical aberration coefficient,  $j_0$  is the cathode current density and  $d$  is the beam diameter at the memory target.

Based on some potential values of the above parameters, these limiting relationships have been plotted on a nomograph as shown in Figure 15. Our measured electron beam readout sensitivities and thus  $M$ , have enabled us to block out the potential performance regions of amorphous semiconductor electron beam memory. They are shown as the hatched regions in Figure 15.

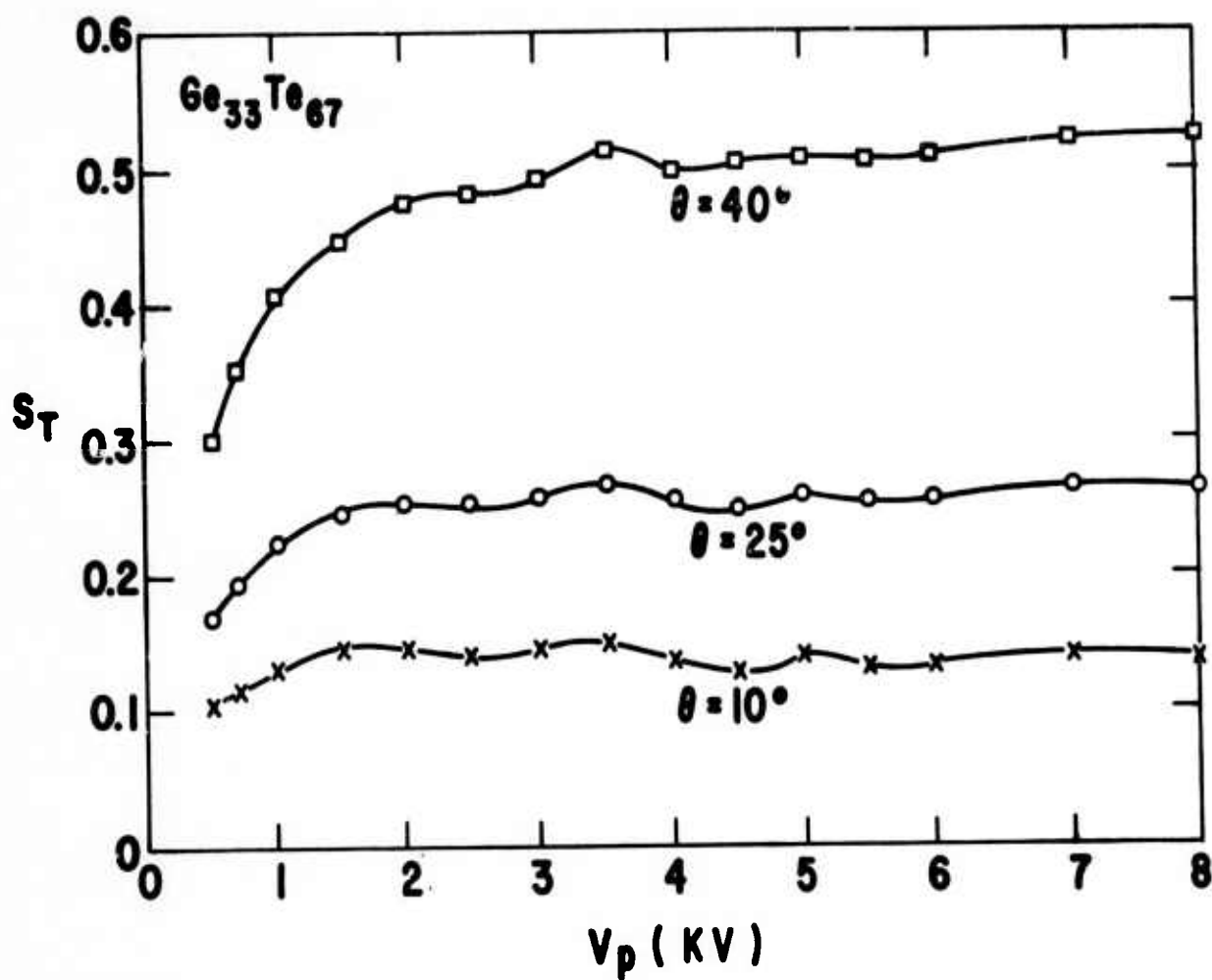


Figure 8 Electron beam readout sensitivity of  $Ge_{33}Te_{67}$  thin films for various surface deformations.

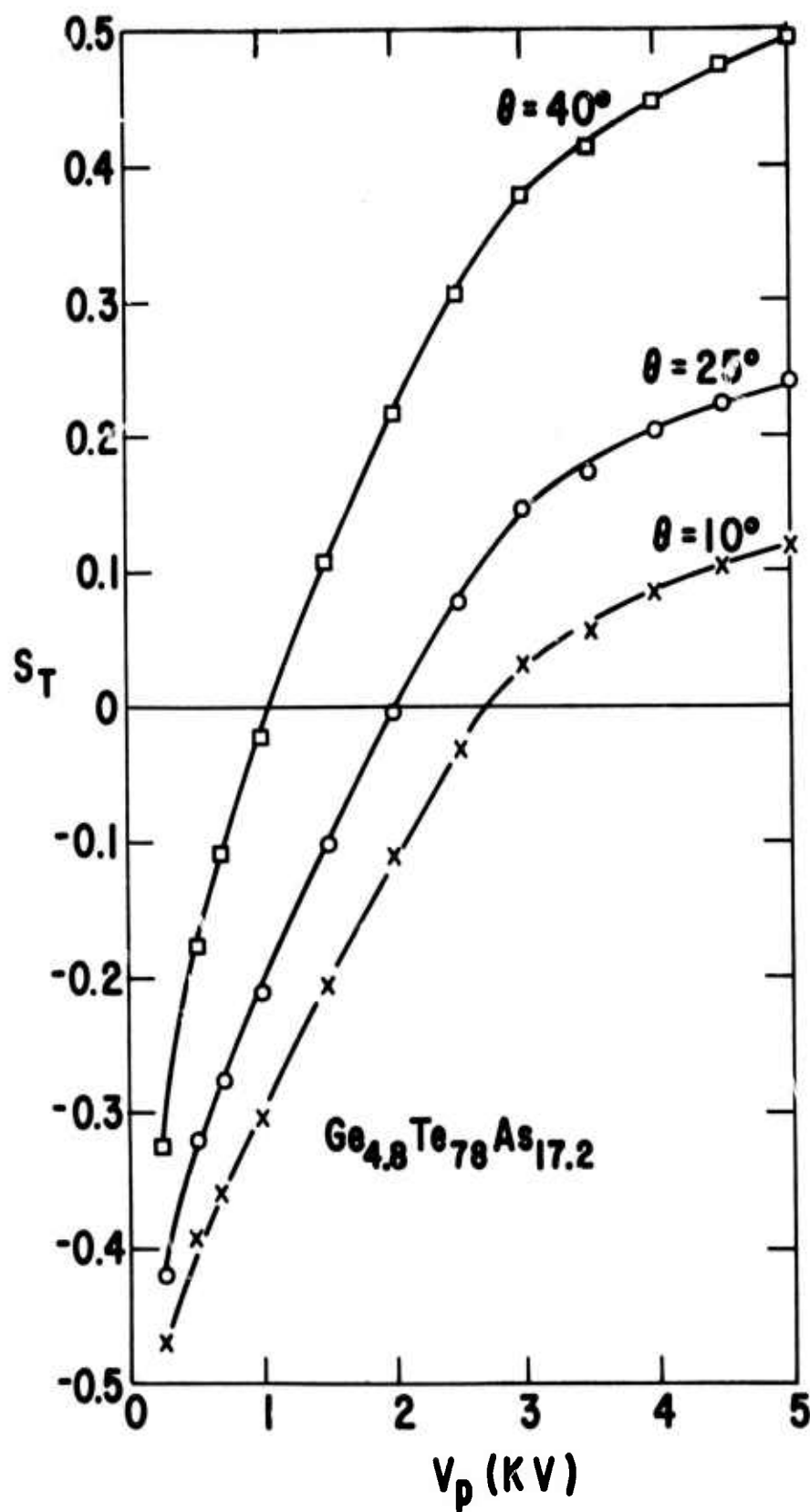


Figure 9 Electron beam readout sensitivity of  $\text{Ge}_{4.8}\text{Te}_{78}\text{As}_{17.2}$  thin films for various surface deformations.

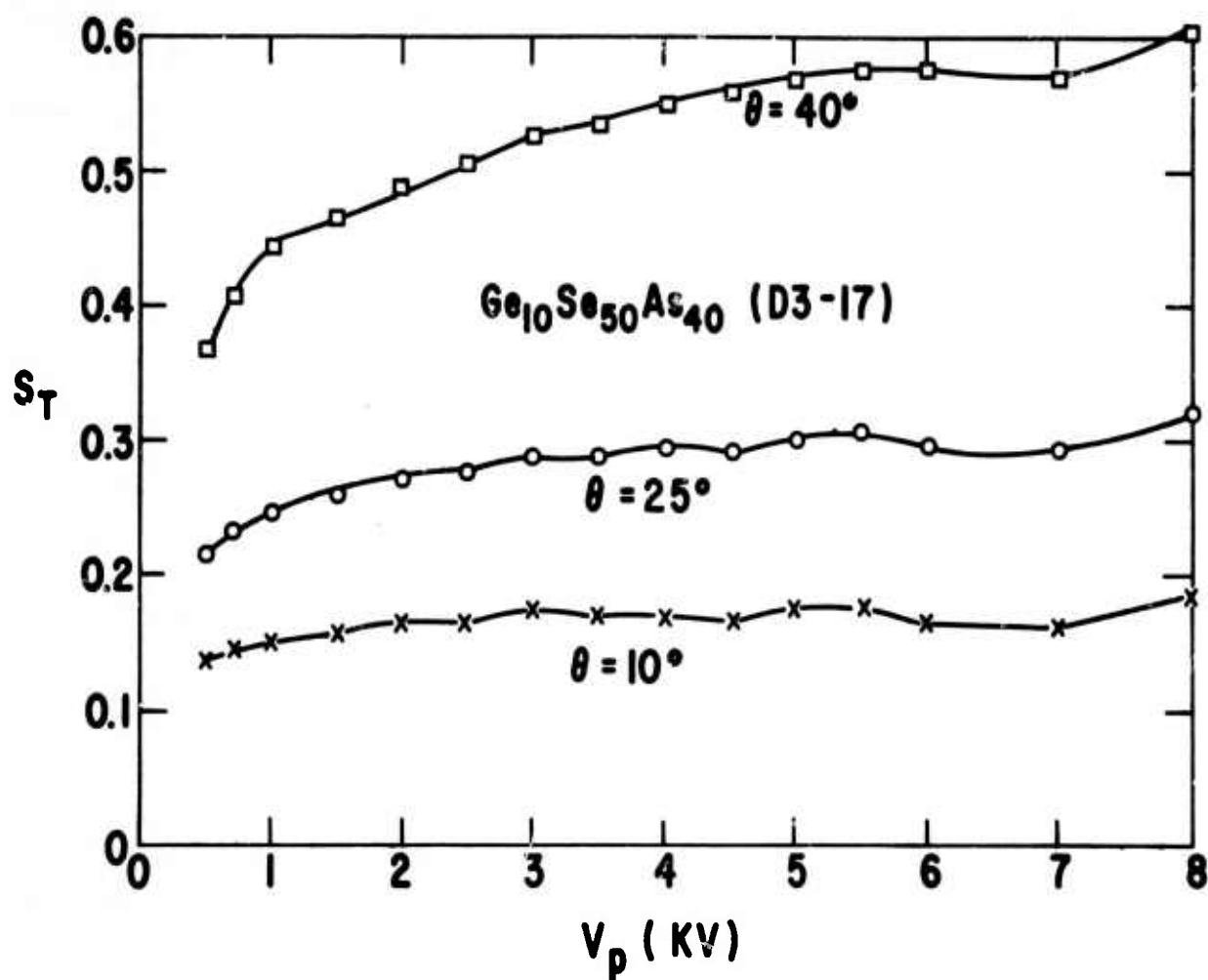


Figure 10 Electron beam readout sensitivity of  $\text{Ge}_{10}\text{Se}_{50}\text{As}_{40}$  thin films for various surface deformations.



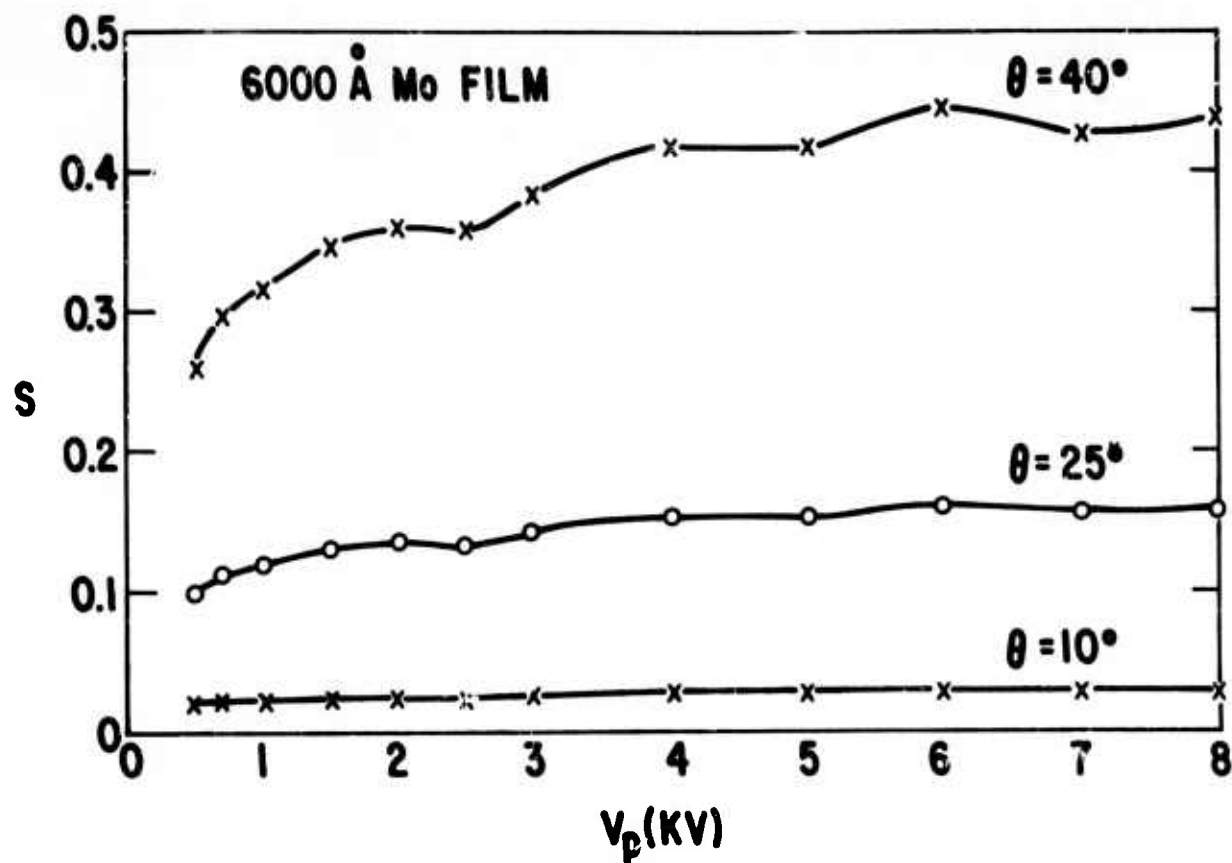


Figure 11 Electron beam readout sensitivity of Mo thin films for various surface deformations.

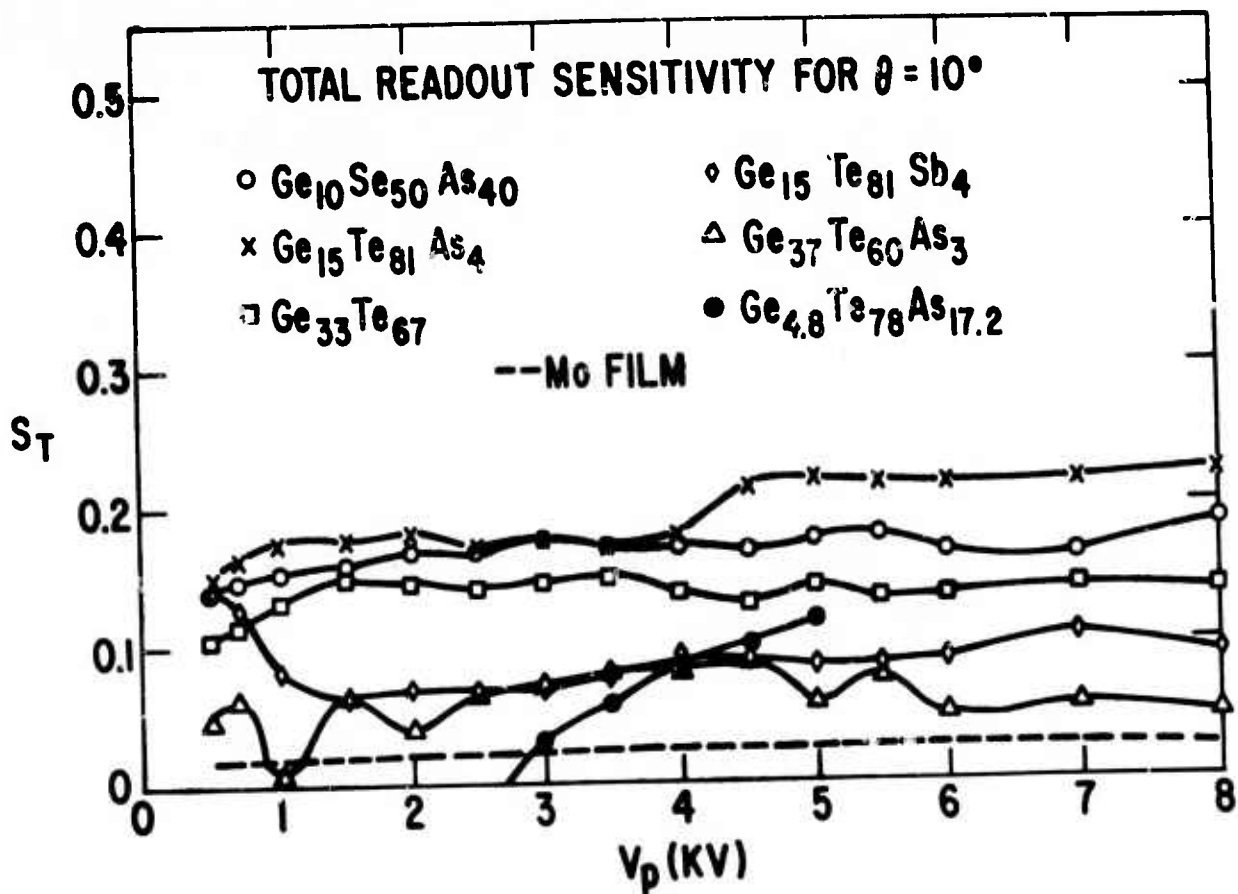


Figure 12 The readout sensitivity of Ge-based thin films for surface deformation of  $10^\circ$ .

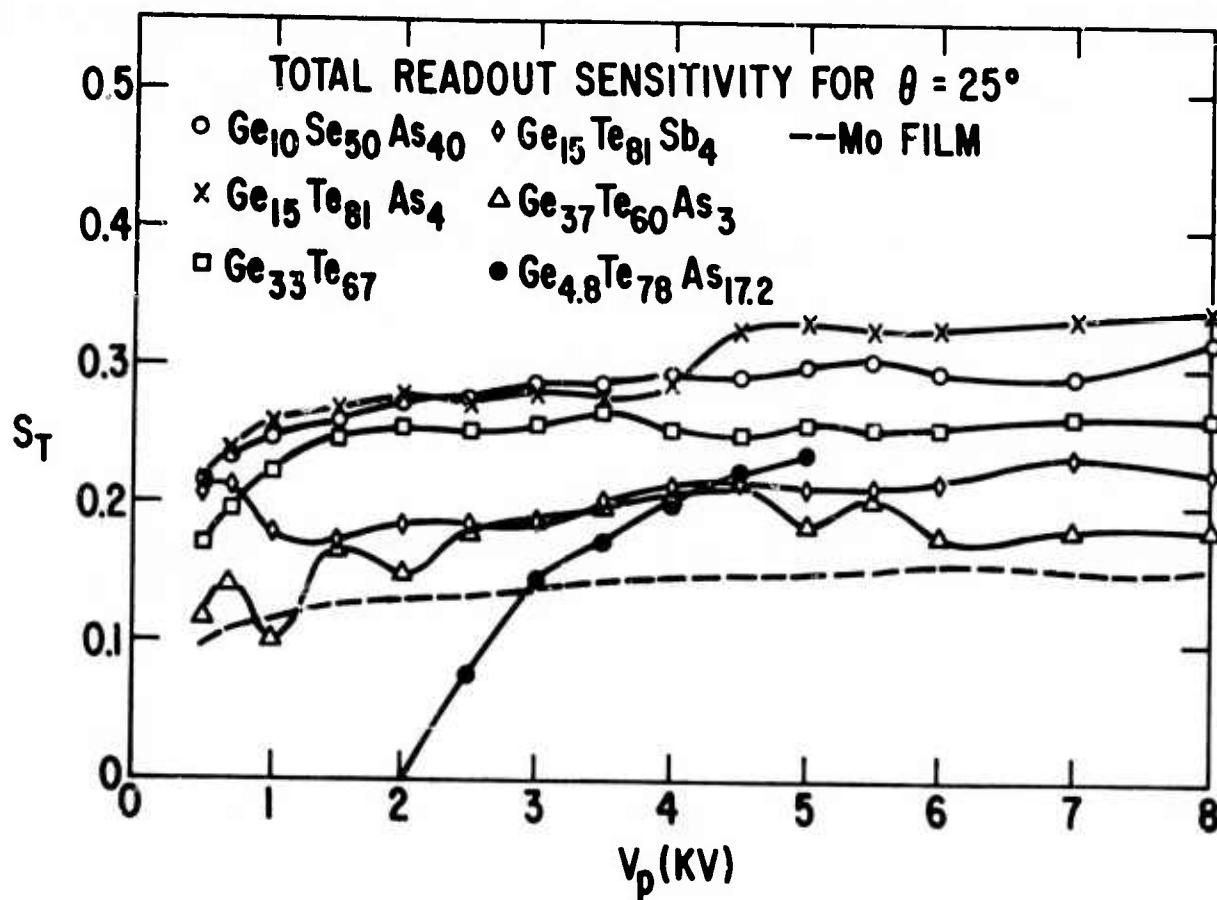


Figure 13 The readout sensitivity of Ge-based thin films for surface deformation of  $25^\circ$ .

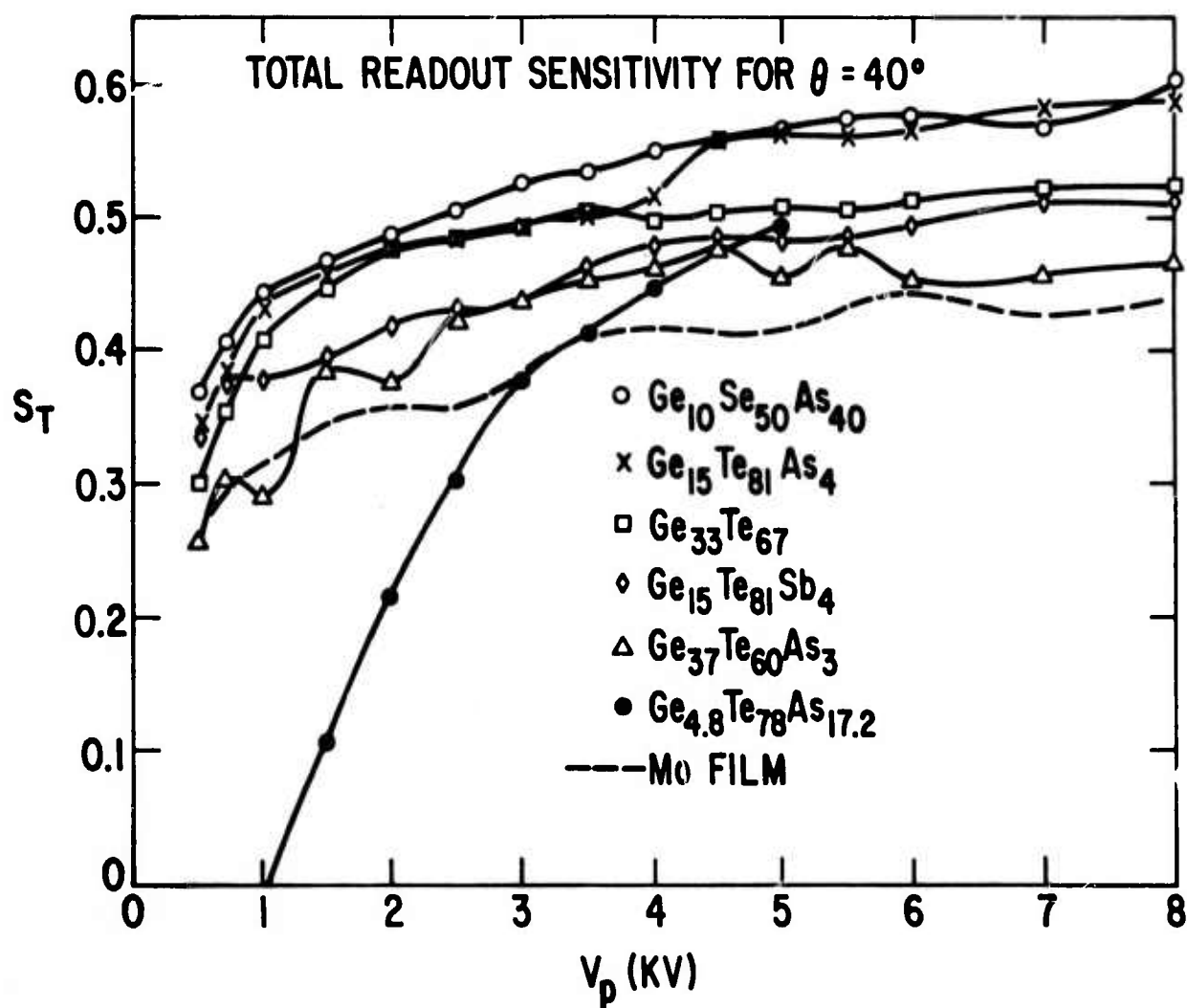


Figure 14 The readout sensitivity of Ge-based thin films for surface deformation of  $40^\circ$ .

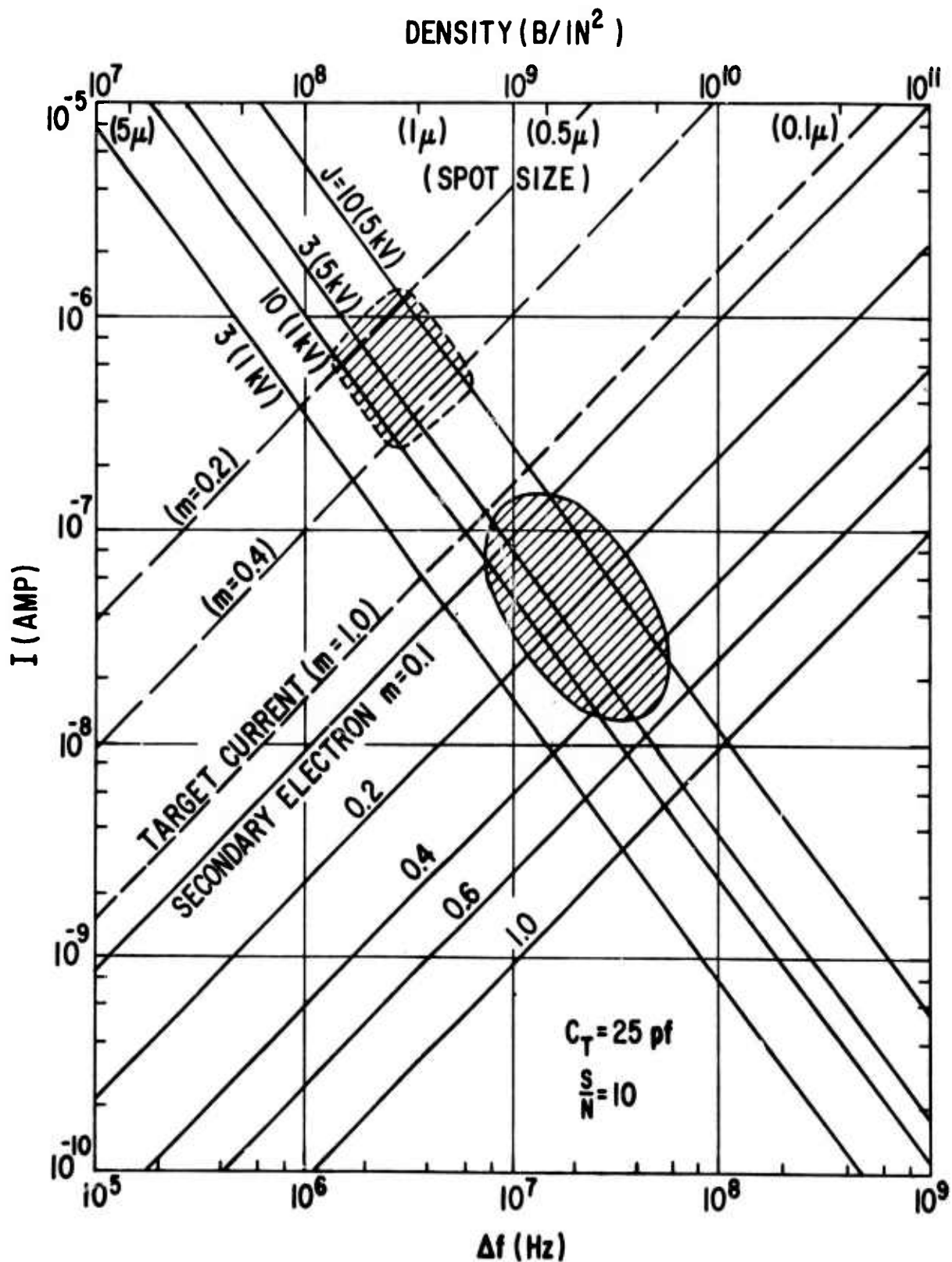


Figure 15 Nomograph of the performance characteristics of amorphous semiconductor electron beam memory. The dashed hatched area is the possible performance region for target readout; the oval hatched region is for secondary electron readout.

### III. A STUDY OF POSSIBLE ELECTRON BEAM ENHANCEMENT OF CRYSTALLIZATION PROCESS IN AMORPHOUS SEMICONDUCTOR THIN FILMS

Our previous investigations have shown that amorphous semiconductors can be crystallized with a high energy electron beam with a duration of 50 ns.<sup>(6)</sup> Lower energy electron beams have induced crystallization in less than 10  $\mu$ s.<sup>(1)</sup> These fast rates as well as the reported photon enhancement of the crystallization process<sup>(8, 9)</sup> strongly suggest that there is a potential electron beam enhancement of crystallization process in these amorphous thin films. Because of the fundamental interest in the physics of amorphous semiconductors as well as the importance of the crystallization phenomenon in electron beam memory we initiated an investigation on possible electron beam enhancement of the amorphous to crystalline transition in Ge-based amorphous film.

#### A. Experimental Technique

Our experimental approach was speculative. It would utilize the crystallization temperature,  $T_x$ , of these thin films as a probe to measure the influence of electron beams on the crystallization process. In essence, we want to determine the change, if any, in  $T_x$  as a function of the incident flux and energy. We have developed a simple and accurate measurement technique of  $T_x$  based on the measurement of thin film resistance vs. temperature. By carefully controlling the sample heating rate we have found that  $T_x$  on selected samples can be measured repeatable to  $\pm 1.5^\circ\text{C}$ . This experimental technique was used successfully in our study of the thickness dependence of  $T_x$  in  $\text{Ge}_{36}\text{Te}_{60}\text{As}_4$  thin films as reported in our second semiannual report.<sup>(5)</sup> Changes of less than  $5^\circ\text{C}$  in  $T_x$  were detected with this technique.

A schematic of the experimental apparatus together with an example of the resultant R vs. T characteristics plotted on the X-Y recorder is shown in Figure 16. At  $T_x$ , there is a sharp decrease (over two orders of magnitude) in the sample resistance within  $5^\circ\text{C}$  span. This sharp decrease enables this experimental technique to determine  $T_x$  to the high precision described above. The details of the experimental apparatus and techniques are described in our second semiannual technical report.<sup>(5)</sup>

To determine the possibility of electron beam enhancement of the crystallization process, the thin film sample would be exposed to intensive electron beam during the heating process. The film's resistance would be monitored continuously by the apparatus described above to detect any effect on  $T_x$ . Rather than comparing the results of two separate measurements; i. e.  $T_x$  with and without beam exposure, it is more accurate to detect the effect by a differential technique. A special thin film sample consisting of essentially two amorphous semiconductor resistors in series were prepared as shown in Figure 17. Only one resistor was exposed to the electron beam. The unexposed resistor was shorter or had lower resistance to assure the

# RESISTANCE vs. TEMPERATURE

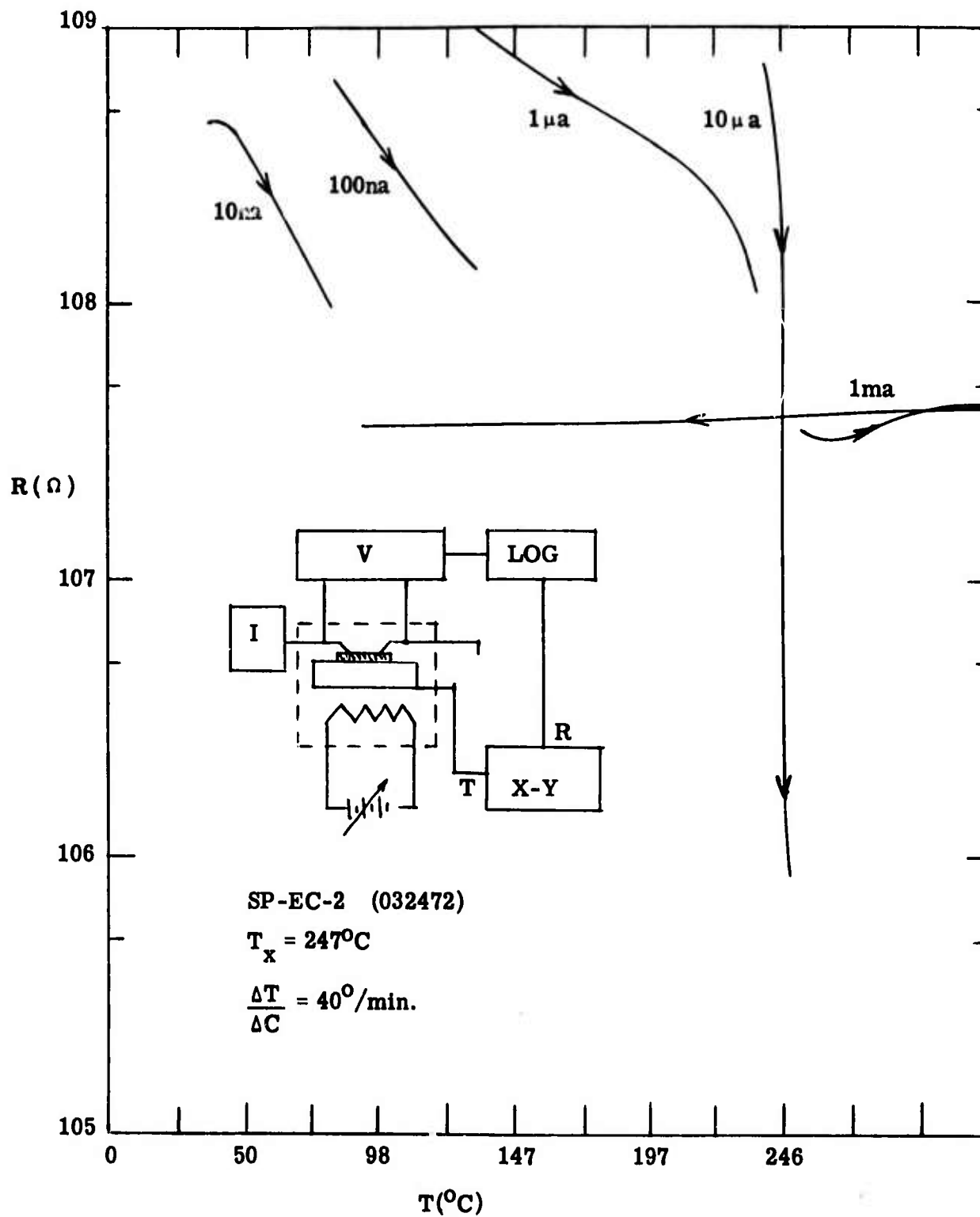


Figure 16 The schematic of the Resistance vs. Temperature measuring apparatus. The measured Log R vs. T curve shows a  $T_x$  of  $276^{\circ}\text{C}$  for this film.

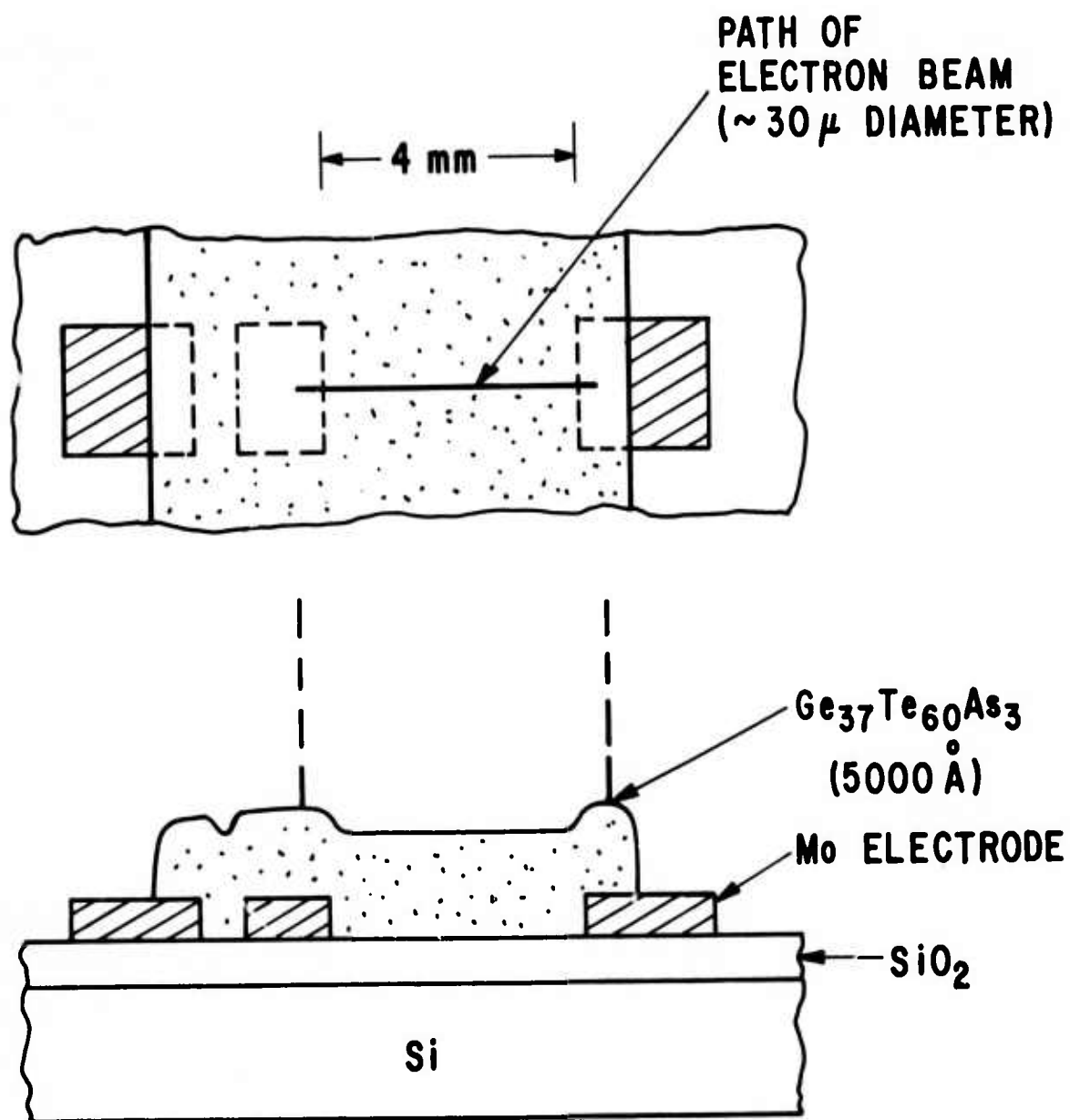


Figure 17 Special amorphous semiconductor thin film resistor structure for electron beam crystallization experiment. Electron is scanned over only the larger of the two series resistors.



detection of the initiation of the crystallization process. Any decrease in  $T_x$  due to electron beam would have resulted in a  $R$  vs.  $T$  plot shown in Figure 18. With electron beam enhancement,  $T_x$  would be decreased resulting in a knee in the  $R$  vs.  $T$  plot.

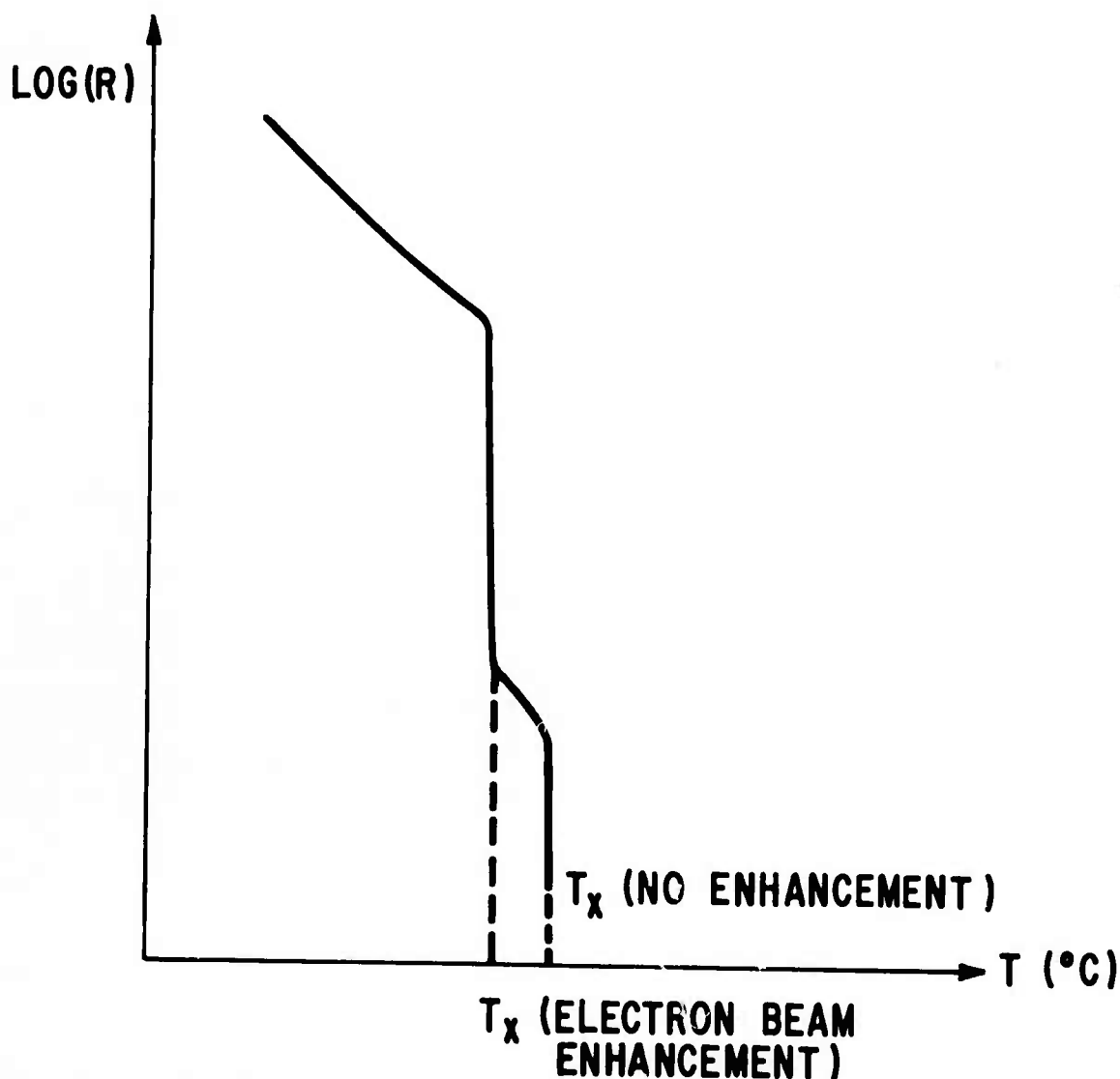


Figure 18 Possible  $\log R$  vs.  $T$  characteristics for electron beam induced decrease in  $T_x$  for sample in Figure 17.

#### B. Electron Beam Test Cell

To carry out the above experiment, we initiated a construction program to improve our electron beam test cell to obtain high brightness and small diameter electron beams needed for our experiment.

The improvements in our electron beam test cell were in three areas:

1. Brighter electron beam source.
2. Lower aberration electron-optic system.
3. High vacuum heated resistance vs. temperature sample stage.

Our original tungsten filament electron source used for our secondary electron emission measurement was inadequate for the planned experiment. A brighter electron source was needed. However, most commercially available brighter sources are susceptible to atmospheric contamination and cannot be used in our open cycle electron beam test cell. Once activated in high vacuum, the emission from these sources rapidly degrade with exposure to the atmosphere. Such sources make careful calibrated measurements difficult. Our solution was a unique high brightness ThC electron source made by General Electric for its own internal use. This source is unaffected by repeated exposure to the atmosphere. The new electron source is shown mounted on the electron beam column in the foreground of Figure 19. The old

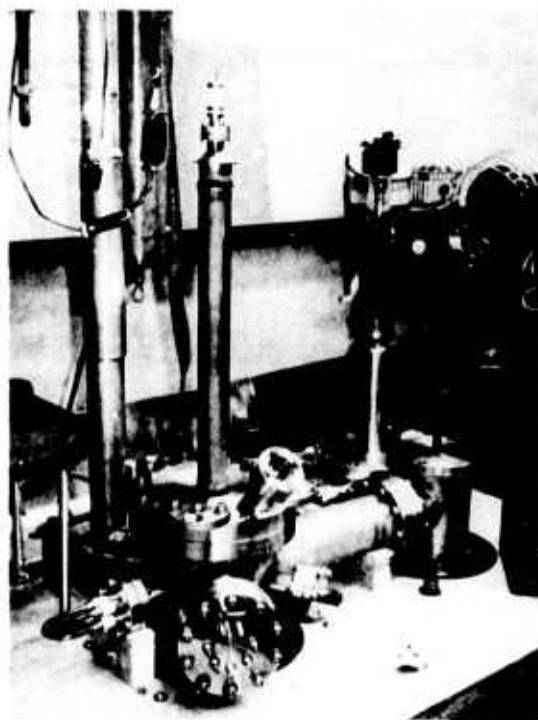


Figure 19 Two electron sources used in this research program. Fore-ground, high brightness ThC electron gun. Background, tungsten filament electron gun.

tungsten electron gun is shown in the background of Figure 19. Unfortunately, the new electron gun did not have a small source diameter, thus our goal of micron diameter electron beam had to be compromised.

The primary cause of aberration in our electron-optic system was identified to be the residue magnetism in the stainless steel electron beam column. To eliminate these aberrations we had hoped to replace the stainless tubing by a ceramic tubing and thus maintain our ultra high vacuum. Unfortunately the joint between this large ceramic tubing and stainless steel flanges was difficult to fabricate and after repeated failures we were forced to use a more fragile glass tubing instead. To maintain the ultra high vacuum the inner surface of the glass tube was coated with a very thin layer of electrodeless nickel rather than the normal aquadag to prevent charge build up. With this precaution we were able to maintain our high vacuum integrity. The electron beam test cell's vacuum was maintained at less than  $10^{-8}$  torr.

With the above two improvements, our electron beam could deliver a beam current of  $2.5 \mu\text{a}$ . The beam diameter was  $25 \mu$  and the beam energy density is about  $7.3 \times 10^5$  watts/cm<sup>2</sup>.

Finally for this experiment, it was anticipated that the electron beam must be capable of high speed modulation. A fast rise time electron beam modulator was designed and constructed using a high speed 10 kv optical isolator. The resultant electron beam system can be modulated with a rise time of 200 ns. The resultant beam waveform using our high speed target current amplifier is shown in Figure 20.

The heated sample stage for the high vacuum resistance vs. temperature measurement is similar to the one described in Ref. (5). However to assure good thermal contact to the heated stage yet maintain excellent electrical isolation, thin ( $1 \mu$ ) thick  $\text{SiO}_2$  films were deposited on the copper heating stage. They can be seen on the surface of the sample stage shown in Figures 21 and 22. The two small circular grids (400 and 200 mesh) in Figure 22 were used to focus our electron beam. The video signal from the 200 mesh grid is shown in Figure 23. As the ratio of the grid bar to spacing is about 1:3, the bar width is about 0.00125" wide. By resolving the flat top of this bar this picture indicated that our beam has about 0.001" or  $25 \mu$  diameter.

The salient improvements in our electron beam test cell necessary for our experiment have been summarized. Aside from these improvements, the electron beam focusing and deflection electronics and other measurements instrumentation have been greatly improved to obtain better electron beam characteristics. The electron beam test cell as an entire system is shown in Figure 24.

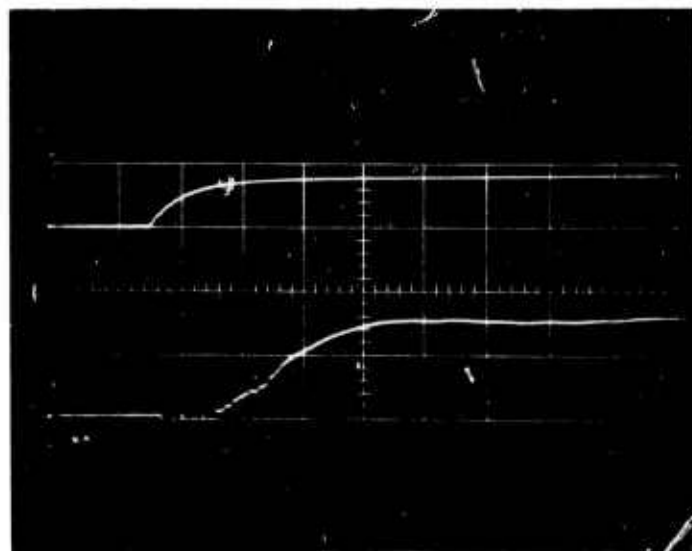
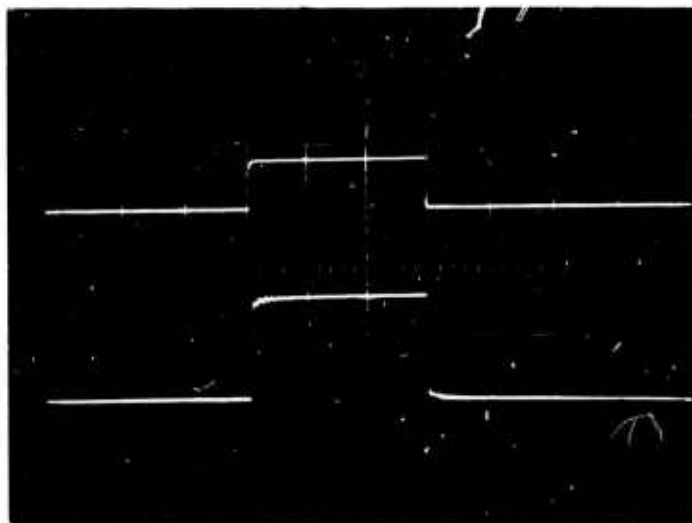


Figure 20 Oscilloscope traces of modulation input (top, 40V) and the electron beam output from target current amplifier (bottom, 2.5  $\mu$ A). Horizontal scale; 5  $\mu$ s/cm (top); 100 ns/cm (bottom).

# HIGH VACUUM RESISTANCE vs. TEMPERATURE MEASUREMENT STAGE

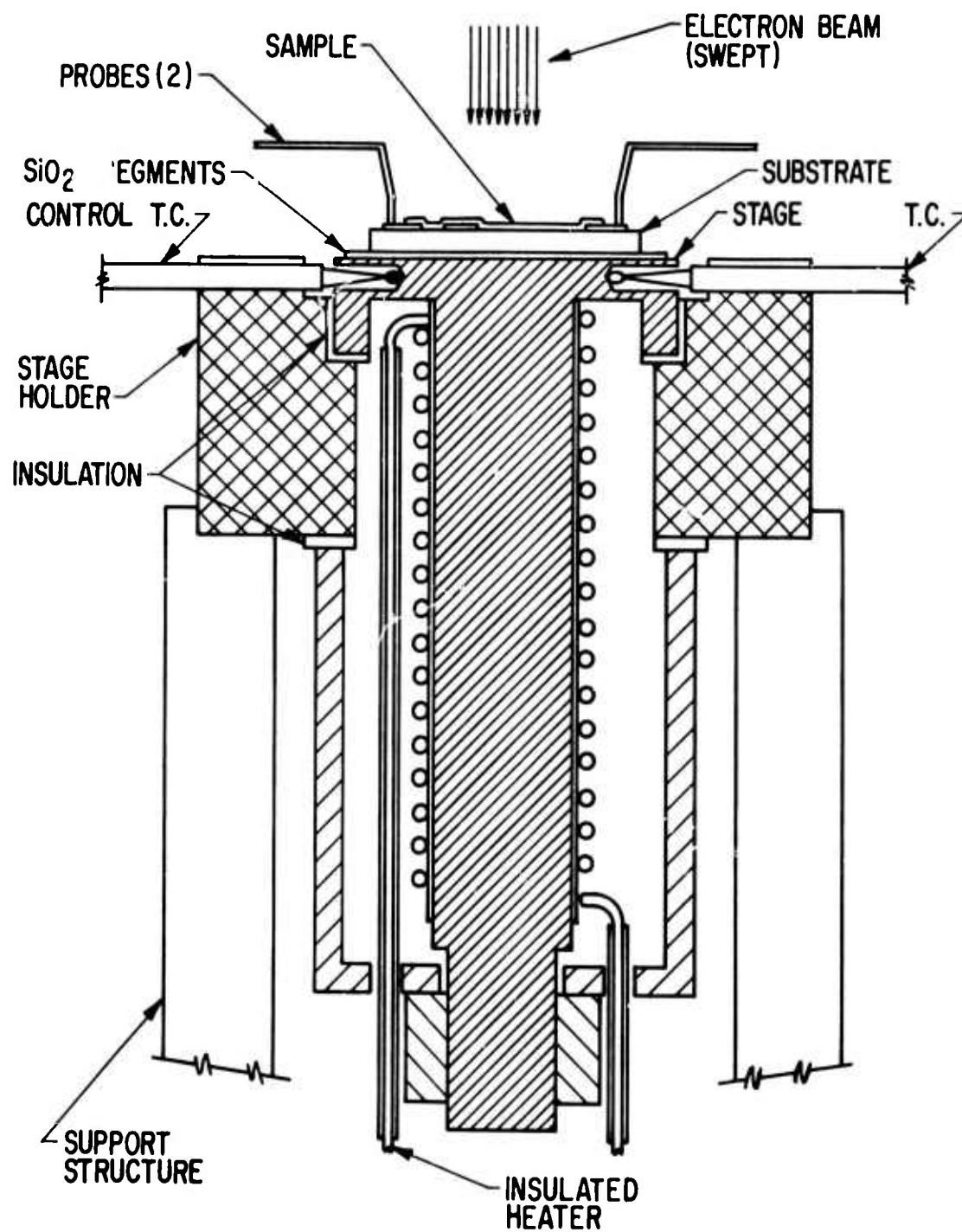


Figure 21 Schematic of the high vacuum heated sample stage for Log R vs. T measurement.

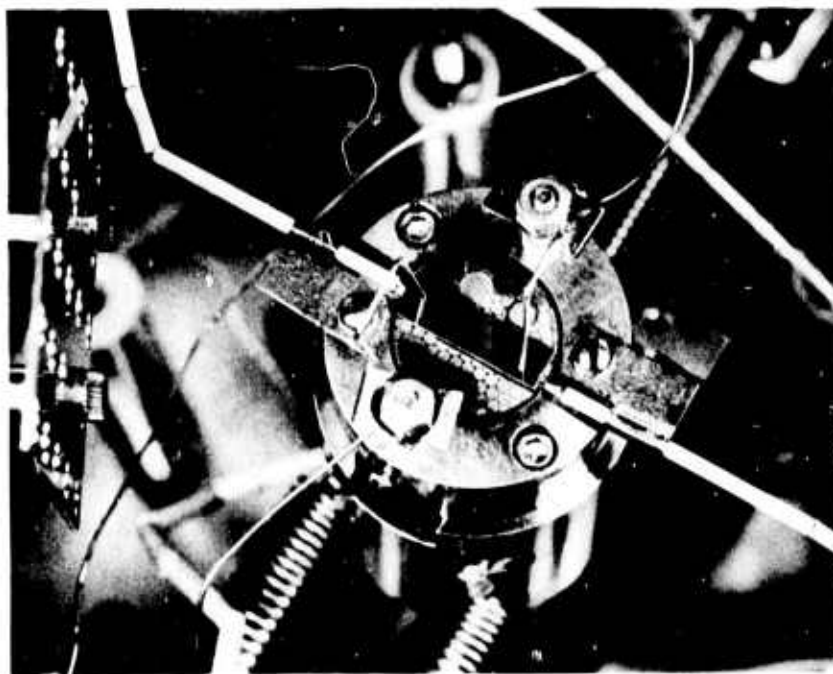


Figure 22 Photograph of the high vacuum sample stage. The two disks next to the resistor sample are the target grids used for electron beam focus adjustment.

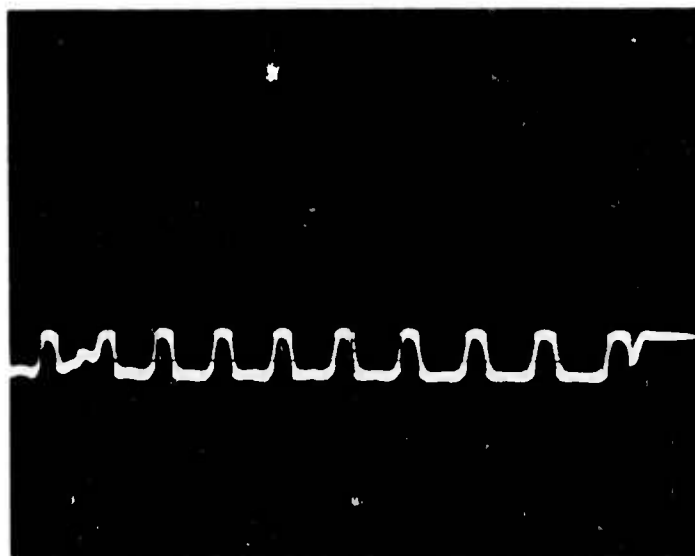


Figure 23 Video signal from the 200 mesh grid used for electron beam focus adjustment.

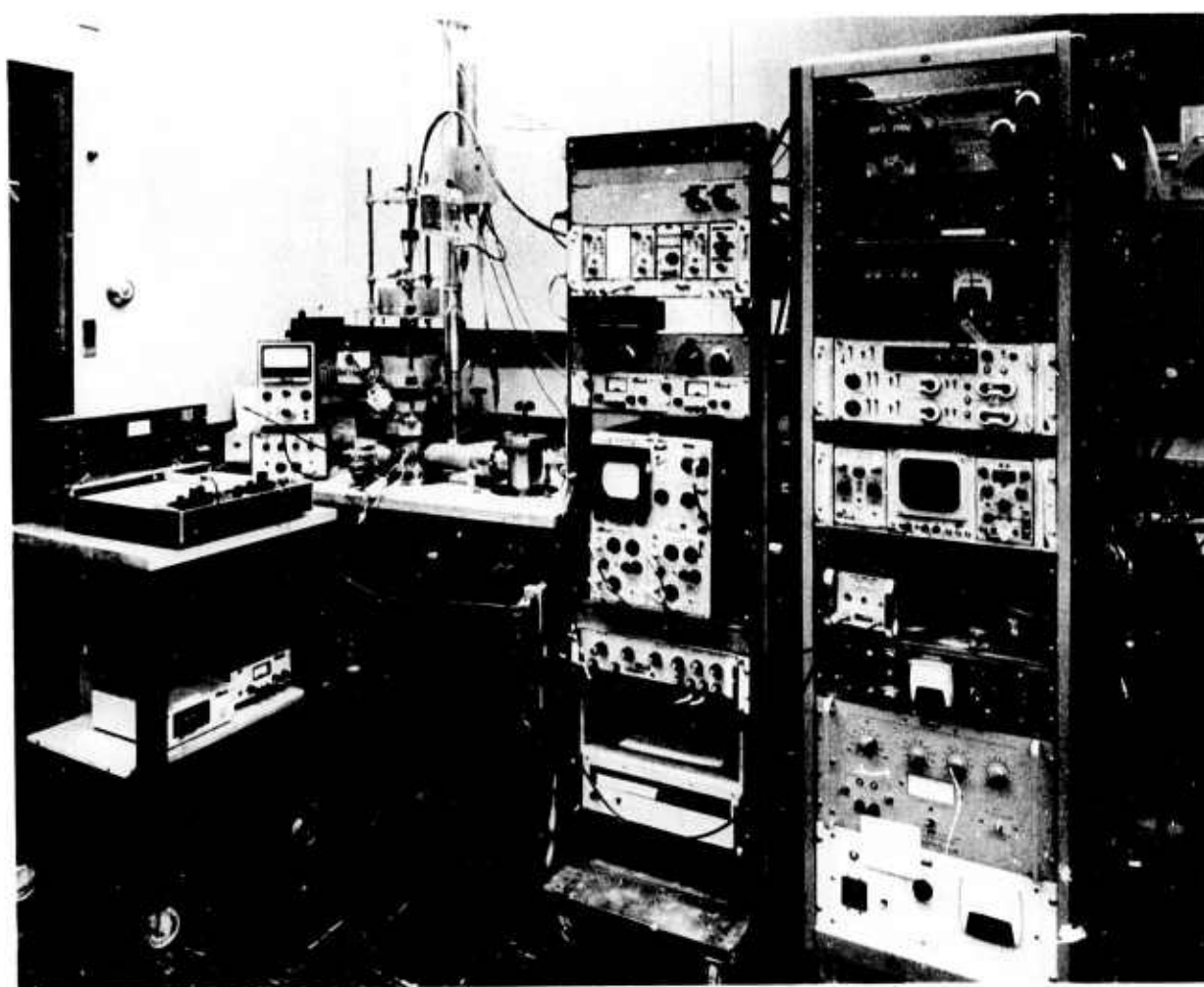


Figure 24 The electron beam test cell with the resistance vs. temperature measurement apparatus.

### C. Experimental Results

$\text{Ge}_{37}\text{Te}_{60}\text{As}_3$  was chosen as our experimental vehicle because of our previous work which has generated a wealth of information on its crystallization behavior. To quickly come to the point, our experimental result was negative. We did not observe any change in  $T_x$  with electron beam exposure.

One problem we encountered was that the small sampling current (10 na - 10  $\mu\text{A}$ ) and the high impedance in our R vs. T apparatus was susceptible to high voltage induced by the intense electron beam. To minimize this effect the 2.5  $\mu\text{A}$ , 6 kv electron beam was scanned over the sample only a small fraction of the time. The period of the scan was 167 ms (60 cycles) while the beam was on for only 5 ms, or 3% of the period. The effective dwell time of the beam was 34  $\mu\text{s}$  per 25 $\mu$  of beam travel. The sample heating rate was about 10°C/min.

This scanning technique had two effects. The first effect is beneficial in that this technique virtually assures no significant electron beam heating of the sample. Thus any observable effect must be due to the electronic nature of the beam. On the other hand, the second effect is the decrease in sensitivity of our experiment. If any effect is due to total integrate electron dosage then our small dosage may not be sufficient to induce any observable effect. Unfortunately, as we did not observe any change in  $T_x$  with electron beam exposure, we can only tentatively conclude that there is no electron beam enhancement of the crystallization process in  $\text{Ge}_{37}\text{Te}_{60}\text{As}_3$  or if there is any, the effect is not a very sensitive process.



INTENTIONALLY LEFT BLANK

#### IV. PARTICIPATING PERSONNEL

A. C. M. Chen

A. M. Dunham

J. M. Wang

#### Publications

- "Interaction of Electron Beam with Amorphous Semiconductor Thin Film",  
A. C. M. Chen, J. M. Wang and J. F. Norton,  
Journal of Non-Crystalline Solids, Vol. 8-10, p. 917 (1972).
- "An Amorphous Semiconductor Electron Beam Memory",  
A. C. M. Chen and J. M. Wang,  
IEEE Transaction on Magnetics, Vol. MAG-8, p. 312 (1972).
- "Electron Beam Heating in Amorphous Semiconductor Beam Memory",  
A. C. M. Chen,  
IEEE Transaction on Electron Devices, Vol. ED-20, p. 160 (1972).
- "Readout Sensitivity of An Amorphous Semiconductor Electron Beam Memory",  
A. C. M. Chen, A. M. Dunham and J. M. Wang  
Journal of Applied Physics, Vol. 44, p. 1936 (1973).
- "Electron Beam Readout Sensitivity of Ge-Te-X Amorphous Thin Films",  
A. C. M. Chen, A. M. Dunham and J. M. Wang  
Presented at the 5th International Conference on Amorphous and Liquid  
Semiconductors, Garmisch - Partenkirchen, Germany, Sept. 1973.
- "An Amorphous Semiconductor Electron Beam Memory",  
Presented at the Government Microelectronics Application  
Conference (GOMAC), San Diego, Calif., October, 1972.

#### References

1. Chen, A. C. M., Norton, J. F., and Wang, J. M., Applied Phys. Lett. 18, 443 (1971).
2. Chen, A. C. M., Norton, J. F., and Wang, J. M., J. Non-Crystalline Solids, 8-10, 917 (1971).
3. Chen, A. C. M., IEEE Trans. on Elec. Dev., ED-20, 160 (1973).

4. Chen, A. C. M. , Dunham, A. M. , and Wang, J. M. , J. Appl. Phys. 44, 1936 (1973).
5. Chen, A. C. M. , "Interaction Between Amorphous Semiconductor Thin Film and Electron Beam", Semiann. Rpt. #2, May, 1973. U.S. Army Contract #DAHC 04-72-C-0016.
6. Chen, A. C. M. and Wang, J. M. , ibid, Semiann. Rpt. #1, Aug. 1972.
7. Chen, A. C. M. and Wang, J. M. , IEEE Trans on Mag. MAG-8, 312, 1972.
8. Dresner, J. , and Stringfellow, G.B. J. Phys. Chem. Solids 29, 303 (1968).
9. Hamada, A. , Kuyosu, T. , Seito, M. and Kikuchi, M. , Appl. Phys. Lett. , 20, 9, (1972).